FULL PAPER

BJC

British Journal of Cancer (2015) 112, 1687–1702 | doi: 10.1038/bjc.2014.586

Keywords: oestrogen; reactive oxygen species; redox regulation; p27; NRF-1; breast cancer

Redox signalling to nuclear regulatory proteins by reactive oxygen species contributes to oestrogen-induced growth of breast cancer cells

V O Okoh[1], N A Garba[1], R B Penney[2], J Das[1], A Deoraj[1], K P Singh[3], S Sarkar[4], Q Felty[1], C Yoo[5], R M Jackson[6] and D Roy*[,1,6]

[1]Department of Environmental and Occupational Health, Florida International University, 11200 SW 8th Street, Miami, FL 33199-0001, USA; [2]Department of Environmental and Occupational Health, University of Arkansas for Medical Sciences, Little Rock, AR 72204, USA; [3]Department of Environmental Toxicology, The Institute of Environmental and Human Health (TIEHH), Texas Tech University, Lubbock, TX 79409, USA; [4]Department of Neuroscience and Cell Biology, UTMB, Galveston, TX 77555, USA; [5]Department of Biostatistics, Florida International University, Miami, FL 33199, USA and [6]Research Service, VA Medical Center, 1201 NW 16th Street, Miami, FL 33125, USA

Background: 17β-Oestradiol (E2)-induced reactive oxygen species (ROS) have been implicated in regulating the growth of breast cancer cells. However, the underlying mechanism of this is not clear. Here we show how ROS through a novel redox signalling pathway involving nuclear respiratory factor-1 (NRF-1) and p27 contribute to E2-induced growth of MCF-7 breast cancer cells.

Methods: Chromatin immunoprecipitation, qPCR, mass spectrometry, redox western blot, colony formation, cell proliferation, ROS assay, and immunofluorescence microscopy were used to study the role of NRF-1.

Results: The major novel finding of this study is the demonstration of oxidative modification of phosphatases PTEN and CDC25A by E2-generated ROS along with the subsequent activation of AKT and ERK pathways that culminated in the activation of NRF-1 leading to the upregulation of cell cycle genes. 17β-Oestradiol-induced ROS by influencing nuclear proteins p27 and Jab1 also contributed to the growth of MCF-7 cells.

Conclusions: Taken together, our results present evidence in the support of E2-induced ROS-mediated AKT signalling leading to the activation of NRF-1-regulated cell cycle genes as well as the impairment of p27 activity, which is presumably necessary for the growth of MCF-7 cells. These observations are important because they provide a new paradigm by which oestrogen may contribute to the growth of breast cancer.

Historically, a majority of breast cancer research has focused on exploring conventional oestrogen receptor (ER) and growth factor pathways with limited investigations on alternative mechanisms of oestrogen action. Redox signalling as an alternative mechanism of oestrogen-dependent breast tumor growth is rapidly emerging with the promise of therapeutic potential. Physiologically achievable concentrations of oestrogen increase reactive oxygen species (ROS) formation in breast cancer cells (Felty *et al*, 2005a; Parkash *et al*, 2006). An increasing body of evidence supports the postulate that oxidative stress generated from exposure to oestrogen, either directly or by influencing the ER, may be an important driver in the development and evolution of human breast cancer (Okoh

*Correspondence: Professor D Roy; E-mail: Droy@fiu.edu

Received 29 July 2014; revised 10 October 2014; accepted 22 October 2014

et al, 2011; Penny and Roy, 2013). The role of ROS in breast cancer is not new; however, a gap in knowledge currently exists with regard to how oestrogen-induced ROS signals nuclear regulatory proteins by way of redox-sensitive proteins. It is widely believed that an impaired redox signalling pathway leads to the dysregulated phosphorylation and/or dephosphorylation of proteins involved in the activation or deactivation of nuclear regulatory proteins (Okoh *et al*, 2011; Penny and Roy, 2013). We have previously shown that 17β-estradiol (E2)-induced DNA synthesis in MCF-7 breast cancer cells depends on mitochondrial oxidant signalling to AP-1, CREB, and NRF-1 (Felty *et al*, 2005a; Parkash *et al*, 2006). This study aims to extend our previous efforts in understanding how an increase in ROS from E2 exposure transduces a signal to nuclear regulatory proteins as well as to identify the key downstream nuclear proteins responsible for the growth of breast cancer cells. We demonstrate for the first time a molecular mechanism of E2-induced activation of NRF-1 leading to the upregulation of cell cycle genes; in addition, the impairment of p27 activity through the ROS-inducible PI3K → PDK1/2 → AKT signal-transduction pathway may be necessary for E2-mediated growth of MCF-7 breast cancer cells.

MATERIALS AND METHODS

Treatment of MCF-7 cells with ROS-scavenging enzymes. The replication-defective, E1- and E3-deleted recombinant (Lam *et al*, 1997) adenovirus-CMV, adenovirus-MnSOD (MnSOD), and adenovirus-catalase (CAT) constructs were purchased from ViraQuest Inc. (North Liberty, IA, USA). MCF-7 cells were seeded in plates at 15–70% confluence. On the following day, cells were infected with different multiplicity of infection (MOI) of MnSOD, CAT, or CMV virus particles in serum-free media (Okoh *et al*, 2013). Infected cells were cultured for 48 h, after which cells were used for experiments. When noted in figure legends, cells were treated by 500 μg ml^{-1} of PEG-CAT.

RNA interference. Predesigned and tetracycline-inducible (Tet-on/off) human shRNA TFAM (mitochondrial transcription factor A) and AKT1 shRNA, pRS shRNA vector, shRNA COPS5 (Jab1), and TrxR2 cDNA were purchased from OriGene Technologies Inc. (Rockville, MD, USA). Predesigned NRF-1 shRNA and corresponding scrambled constructs were purchased from Ambion (Morrisville, NC, USA). Transfections of cells were carried out in a subconfluent MCF-7 cell population using FuGENE 6 (Promega, Madison, WI, USA). Transfection efficiencies ranged between 60 and 80% as quantified by decreased protein expression levels. MCF-7 cells were transfected with Tet-on/off TFAM shRNA in serum-free media for 48 h, after which cells were treated with vehicle (dimethyl sulfoxide (DMSO)) or E2 (367.1 pM) for 24 h. Mitochondrial transcription factor A expression was turned on by the addition of 0.5 μg ml^{-1} doxycycline. Western blots were probed with antibodies against TFAM and β-actin as a loading control to verify the knockdown of TFAM protein level. For shRNA knockdown of AKT expression, cells were transfected with predesigned and verified human shRNA for AKT1 and control shRNA plasmid consisting of scrambled shRNA sequence that does not lead to the specific degradation of AKT1 (OriGene Technologies Inc.). NRF-1 silencing cells were transfected with predesigned and verified human shRNA for NRF-1 and control shRNA plasmid consisting of scrambled shRNA sequence that does not lead to the specific degradation of NRF-1. Cells were also treated with Jab1 shRNA and control shRNA plasmid consisting of scrambled shRNA sequence that does not lead to the specific degradation of Jab1 (OriGene Technologies Inc.).

Colony formation assay. MCF-7 cells were seeded in six-well plates with a bottom layer of 0.7% agar in DMEM/F12 and cells were seeded on top in soft agar (0.3%) made in steroid-free medium containing DMSO as a vehicle or E2 (367.1 pM), or hydrogen peroxide (H_2O_2) (5, 25, or 600 μM) with and without ROS or other modifiers (Okoh *et al*, 2013). Cells were fed weekly with soft agar (0.3%) layer. Colony formation was recorded at different time intervals after treatment, when cell masses grew to 100 μm or greater as measured by a Nikon TE2000U inverted microscope (Melville, NY, USA).

Determination of ROS. MCF-7 cells were seeded at a concentration of 1.0×10^4 cells per well in 96-well plates and pretreated for 4 h with chemical antioxidants such as 20 μM ebselen (a glutathione peroxidase mimic) or 1 mM *N*-acetylcysteine (NAC) followed by treatment with E2 (367.1 pM), 1 μM tamoxifen (TAM) citrate (Sigma, St Louis, MO, USA), or vehicle (DMSO) for 30 min. Production of ROS was determined in MCF-7 cells treated with E2 (367.1 pM) in the presence or absence of ROS modifiers. MCF-7 cells overexpressing MnSOD and CAT or pretreated with ROS scavengers ebselen or NAC for 4 h. MCF-7 cells were serum starved for 48 h and pretreated with 10 μM of 2′, 7′-dichlorofluorescein-diacetate (DCFH-DA) (Molecular Probes, Eugene, OR, USA) for 20 min followed by treatment with E2. 2′, 7′-Dichlorofluorescein-diacetate is a non-fluorescent cell-permeable compound, which is acted upon by endogenous esterase that remove the acetate groups generating DCFH. In the presence of intracellular ROS, DCFH is rapidly oxidised to the highly fluorescent 2′, 7′-dichlorofluorescein (DCF). The oxidative products were measured with a Tecan Genios microplate reader (Morrisville, NC, USA) using 485 and 535 nm excitation and emission filters, respectively, as previously described by Felty *et al* (2005a). Reactive oxygen species was also determined by a confocal microscopy. The oxidation of ROS-sensitive dye DCFH-DA and labelling mitochondria with MitoTracker Red were used to show ROS formation in mitochondria of MCF-7 cells treated with TAM.

BrdU cell proliferation assay. Bromodeoxyuridine (BrdU) incorporation was determined as a biological indicator of DNA synthesis in MCF-7 cells treated with E2 (367.1 pM) in the presence or absence of ROS modifiers. MCF-7 cells overexpressing MnSOD and CAT or pretreated with ROS scavengers ebselen (20 μM) or NAC (1 mM) for 4 h were exposed to E2 for 48 h before BrdU incorporation. MCF-7 cells were grown (2500 cells per well) in 96-well plates until 50% confluent in 10% FBS DMEM/F12, and then serum starved for 48 h followed by the treatment. Cells were pretreated for 4 h with ROS scavengers 20 μM ebselen or 1 mM NAC followed by treatment with E2 (367.1 pM). Next, cells were labelled with BrdU for 24 h. Afterwards, a colorimetric BrdU cell proliferation assay was performed according to the manufacturer's instructions (Roche, Branford, CT, USA) as described previously (Felty *et al*, 2005b). Absorbance of the samples was measured in a Tecan Genios microplate reader at 450 nm (reference λ at 700 nm).

Cell viability and ATP assays. Cell viability was measured using the CellTiter-Fluor Cell Viability Assay Kit (Promega), which measures conserved constitutive protease activity in live cells. Quantitation of the ATP present in the MCF-7 cells exposed to vehicle (DMSO) or E2 (367.1 pM) for 0.5 and 16 h was carried out by recording the luminescence of CellTiter-Glo Reagent (Promega).

Electrophoretic mobility shift assay. Electrophoretic mobility shift assay (EMSA) was performed with DIG-11-ddUTP 3′-end labelled probes. The oligonucleotide sequences used for EMSA were as follows: the NRF-1 consensus sequence from human TFA promoter region (NRF-1 forward primer, 5′-CGCTCTCC CGCGCCTGCGCCAATT-3′; NRF-1 reverse primer, 5’-GGGCGG AATTGGCGCAGGCGCGGG-3′). Probe labelling and binding reactions were performed using the DIG Gel Shift Kit (Roche) following the protocols provided by the manufacturer as described

previously (Felty *et al*, 2005a). Nuclear extracts were collected and 5 μg of extract was loaded for all samples. Samples were electrophoresed on a 6% native polyacrylamide gel and transferred to a nylon membrane by electroblotting. Binding was detected by chemiluminescent detection as described in the DIG Gel Shift Kit protocol (Roche). A competitive binding reaction with 100-fold higher concentration of unlabelled oligos as compared with labelled oligos in both vehicle (DMSO) and E2 treatments served as the negative control.

Antibodies and immunoblotting analysis. Lysates from MCF-7 cells overexpressing MnSOD and CAT or pretreated with ROS scavengers ebselen (20 μM) or NAC (1 mM) for 4 h were exposed to E2 (367.1 pM) for 30 min before being processed for western blotting and were probed with the following antibodies ERK1/2, p-ERK1/2, p27, p27(T157)-P, ERα, p-ERα, Jab1, TFAM, PTEN, or CDC25A (Santa Cruz, Dallas, TX, USA), anti-NRF-1 (Rockland, Limerick, PA, USA), phosphorylated AKT (p-AKT) (Ser 473) and total AKT antibodies (Cell Signaling), GAPDH, or β-actin (Sigma). For immunoprecipation experiments, total cell lysates of DMSO- or E2-treated (367.1 pM for 30 min) MCF-7 cells were immunoprecipitated (IP) with anti-NRF-1 or anti-CDC25A antibodies, and immunoblots were probed with anti-NRF-1, anti-AKT, antiphosphoserine, or antityrosine antibodies.

Redox western blot analysis. MCF-7 cells (1×10^6) seeded into 100 mm plates were pretreated with 10 μM erucin for 48 h followed by DMSO or E2 (367 nM) treatment for 30 min. A total of 50 μg protein was resolved by 15% SDS–PAGE under non-reducing conditions subjected to immunoblot analysis using anti-Trx and β-actin antibodies as previously described by Watson *et al* (2003).Total proteins were resolved by 15% SDS–PAGE under non-reducing conditions and were detected using an anti-Trx antibody. Steady-state redox potential (Eh, redox state) was calculated using the Nernst equation (EoTrx1 = -240 mV, pH 7.4), as described by Watson *et al* (2003). Protein bands corresponding to reduced and oxidised forms of Trx were recorded on X-ray films or as Versadoc images and then subjected to densitometry analysis using the ImageJ software. Quantified protein band intensities of oxidised and reduced Trx bands were used for the calculation of EhTrx and the steady-state redox potential. The oxidised state of PTEN was detected by EMSA using the alkylating agent *N*-ethylmaleimide, by in MCF-7 cells. In brief, the oxidation state of PTEN was investigated using alkylating agents, in cell lysates from E2 (367 nM) or TAM (1 μM) for 30 min and untreated cells grown in the absence and presence of 10 mM ebselen. Total protein lysates were resolved by 10% SDS–PAGE under non-reducing conditions. Reduced and oxidised forms of PTEN were detected by immunoblot analysis with rabbit anti-PTEN. To assess the cysteine oxidation in CDC25A by E2-induced ROS, lysates from E2-treated cells (367 nM) for 30 min and untreated cells grown in the absence and presence of 10 mM NAC were labelled with a sulphydryl-specific reagent 5-iodoacetamidofluorescein (5-IAF), obtained from Pierce (Rockford, IL, USA) using the protocol of Wu *et al* (1998), IP with anti-CDC25A, and detected using rabbit antifluorescein. Immunoglobulin G level was used as a loading control of each IP sample.

Assay of CDC25A phosphatase activity. CDC25A phosphatase activity was measured at pH 7.4 and at ambient temperature with the artificial substrate O-methylfluorescein phosphate (OMFP) in a 96-well microtiter plate assay based on the method described by Lazo *et al* (2001). MCF-7 cells were lysed and IP with phosphoserine agarose-coupled antibodies followed by western blotting with anti-CDC25A antibodies. The total cell lysate was analysed for CDC25A phosphatase activity using OMFP as the substrate.

***In vitro* kinase assays.** Recombinant human NRF-1 (50 ng) alone or in combination with 1 μg recombinant human AKT was incubated in 30 μl kinase buffer with or without 200 μM ATP for 10 min at 30 °C. Cell lysates were subjected to 8% SDS–PAGE and probed with anti-phosphoserine and anti-NRF-1 antibodies.

Identification of NRF-1 phosphorylation sites by mass spectrometry. Several AKT phosphotyrosine sites were detected by tandem mass spectrometry (MS/MS) methods. Tandem mass spectra were searched against the reversed and concatenated Swiss-Prot protein database using the Sequest algorithm (Proteomics browser; Thermo Scientific, Rockford, IL, USA) with differential modifications for STY phosphorylation ($+79.97$) and methionine oxidation ($+15.99$). Phosphorylation sites were identified if they initially passed the following Sequest scoring thresholds. Determination of the exact sites of phosphorylation was aided using the GraphMod software (Proteomics browser; Thermo Scientific).

Immunofluorescence staining. The fluorescent probe Mito-Tracker Red was used for labelling of mitochondria (fluorescence intensity as a surrogate for mitochondrial mass). Images of MitoTracker Red 580 incorporation in mitochondria ($\times 40$) were acquired by fluorescence confocal microscopy after 15 min of adding E2 or DMSO, as described by Parkash *et al* (2006). MCF-7 cells were seeded and treated in chamber slides. After E2 treatment, cells were fixed with ice-cold methanol for 15 min, and permeabilised with 0.5% Triton X-100 for 30 min. Cells were then incubated with primary antibodies and Alexa Fluor-conjugated secondary antibodies. The confocal fluorescence images were scanned on a Nikon TE2000U inverted microscope. The fluorescent probe MitoTracker Red was used to label mitochondria and its fluorescence intensity was monitored as an indirect measure of mitochondrial mass. Images of MitoTracker Red 580 incorporation in mitochondria were acquired by fluorescence confocal microscopy after 15 min of adding E2 or DMSO, as described previously (Parkash *et al*, 2006). The confocal images were acquired on a Nikon C1 laser scanning confocal microscope (Melville, NY, USA). *In vivo* phosphorylation of endogenous NRF-1 by E2 treatment was determined by immunofluorescent labelling with Alexa Fluor 488-mouse anti-phosphoserine and NRF-1-anti-rabbit antibodies (Alexa Fluor 633-conjugated secondary antibody). *In vivo* phosphorylation of ER by E2 treatment was determined by immunofluorescent labelling. *In vivo* phosphorylation of p27 by E2 treatment was determined by immunofluorescent labelling. MCF-7 cells were stained with immunofluorescent p27 and p27(T157)-P antibodies and conjugated with Alexa Fluor 488 and 635-labelled secondary antibody conjugates, respectively, and analysed by confocal microscopy for localisation of p27Kip1 and p27(T157)-P. For semiquantitation, p27-, p27(T157)-P-, ERα-, and p-ERα-immunopositive cells, in which >300 cells were counted in three independent experiments.

ChIP qPCR to analyse NRF-1 binding to the promoters of cell cycle genes. Chromatin immunoprecipitation assays (ChIP) were carried out with the ChIP Assay Kit (Upstate Biotechnology, New York, NY, USA). MCF-7 cells (3×10^6) overexpressing MnSOD or CAT were treated with either E2 (367.1 nM) for 16 h or analysed by ChIP assay using the anti-NRF-1 antibody. DNA from chromatin IP with anti-NRF-1 antibodies was amplified with primers specific for the PRC1, CDC2, PCNA, cyclin B1, and CDC25C promoter region containing NRF-1 sites using an ABI Biosystem 7300 thermocycler (Grand Island, NY, USA) with the following cycle conditions: initial 10 min at 95 °C followed by 40 cycles of 95 °C, 15 s and 60 °C, 60 s. Chromatin immunoprecipitation qPCR results were calculated using the $\Delta\Delta$Ct method.

Real-time qRT–PCR analysis. Total RNAs were isolated with TRIzol reagent (Life Technologies, Grand Island, NY, USA) from MCF-7 cells exposed to E2 for 16 h in the presence and absence of ROS modifiers using the ChIP assay condition. The RNA templates were reverse transcribed into cDNA using reverse transcription reagents with random hexamer primers (Applied Biosystems, Grand Island, NY, USA). The cDNA was then used as the template for real-time PCR with gene-specific primers. The TaqMan primers of PRC1, CDC2, PCNA, cyclin B1, CDC25C, and 18S were used. Quantitative gene expression analysis was performed by TaqMan-based qRT – PCR on ABI 7700 (PE Applied Biosystems, Foster City, CA, USA).

RESULTS

ROS-scavenging enzymes suppress E2-induced DNA synthesis of MCF-7 cells. Our previous studies have shown that mitochondria are a major site of E2-induced ROS in breast cancer cells (Felty *et al*, 2005a; Parkash *et al*, 2006). The specific individual ROS that is most relevant to E2 signalling pathophysiology has yet to be identified. As the antioxidants ebselen and NAC are nonspecific in the type of ROS scavenged, we chose to overexpress antioxidant enzymes. The mitochondrial antioxidant enzyme MnSOD dismutates $O_2^{\bullet -}$. Therefore, we determined whether increased formation of $O_2^{\bullet -}$ signalled E2-induced DNA synthesis by overexpressing MnSOD. Within the mitochondria, MnSOD can dismutate $O_2^{\bullet -}$ to H_2O_2, which is a highly diffusible signalling molecule that can exit the mitochondria. Thus, we also determined whether increased H_2O_2 formation signalled E2-induced DNA synthesis by overexpressing CAT. We used intracellular DCFH-DA oxidation method to measure the endogenous ROS levels in the MCF-7 cells exposed to an E2 concentration equivalent to the physiological and pharmacological levels in the target tissue (367.1 pM) for 30 min in the presence or absence of ROS scavengers. As expected, E2 treatment induced significantly more ROS in MCF-7 cells compared with vehicle control. The ability of E2 to produce ROS was prevented by treatment with chemical ROS scavengers ebselen or NAC (Figure 1A). Both ebselen and NAC inhibited E2-induced BrdU incorporation in the MCF-7 cells. These findings are in agreement with our previous studies (Felty *et al*, 2005a, b). When MnSOD was overexpressed in MCF-7 cells, ROS levels increased significantly compared with cells with empty vector (CMV). 17β-Oestradiol-exposed MCF-7 cells transduced with MnSOD at an MOI of 200 or 200 virus particles showed a 400% increase in ROS production and less BrdU incorporation compared with control cells (Figure 1B). 17β-Oestradiol-exposed MCF-7 cells transduced with CAT at an MOI of 200 produced 130% less ROS and incorporated less BrdU compared with E2-treated MCF-7 cells with the vector alone (Figure 1B). We also measured cellular protease activity to rule out the possibility that the changes in ROS levels were not as a result of different cell densities or viability. There was no change in protease activity between MCF-7 cells transduced with MnSOD and CAT or empty CMV vector adenoviral constructs (data not shown). These findings further support that H_2O_2 and $O_2^{\bullet -}$ have an important role in E2-mediated growth of breast cancer cells.

ROS modifiers modulate E2-induced colony-forming activity of MCF-7 breast cancer cells. As long-term (21 days or longer) survival of colonies in semisolid media is considered an important phenotypic property of most cancer cells (Aapro *et al*, 1987) and strongly correlates with tumorigenicity in experimental animals, we reasoned that if E2 is responsible for the promotion and progression of breast tumor, then ROS may also contribute to colony-forming phenotypic ability of MCF-7 breast cancer cells. Therefore, we used the clonogenic assay instead of monolayer liquid cell culture to monitor whether E2-induced ROS promoted the ability of MCF-7 cells to form colonies. As expected, the ability of MCF-7 to form colonies on soft agar was significantly higher in E2-treated cells (100 pg ml^{-1} for 21 days) compared with control cells. Treatment of cells with ROS scavengers (20 μM ebselen or 1 mM NAC) significantly inhibited colony formation in E2-treated MCF-7 cells (Figure 1C). MCF-7 cells overexpressing CAT (protein levels confirmed by western blot) produced lower levels of ROS and fewer colonies when compared with E2-treated cells with vector alone (Figure 1D). This implies that when ROS levels were diminished by biological or chemical modifiers, E2-induced colony formation of MCF-7 cells was inhibited. However, this phenomenon was not observed in MnSOD-overexpressing cells. As shown in Figure 1B, MCF-7 cells transduced with MnSOD at an MOI of 200 showed a significant increase of ROS production and reduced MCF-7 colony formation in E2 treatment (Figure 1D). We observed that MCF-7 cells treated with MnSOD at an MOI of 5–50 showed an increased number and size of colonies, whereas an MnSOD dose >50 MOI diminished MCF-7 colony formation (Figure 1E and F). The adenovirus-containing control vectors (50 MOI) did not produce any growth advantage compared with wild-type MCF-7 cells. The observed reduction of MCF-7 cell growth by treatment with MnSOD >50 MOI was not because of cell death, as we found that over 70% of adenoviral-infected cells were viable up to a dose of 200 MOI based on the Trypan blue assay, whereas 90% of the cells treated with MnSOD at 400 MOI were not viable at 21 days of culture in soft agar assay (data not shown). The suppression of the number and size of MCF-7 colonies were dependent on the MOI of the adenoviral constructs containing MnSOD, CAT or CMV. Our data showed that when cells were treated at lower MOI of MnSOD, the number and size of colonies increased, while at higher MOI both parameters in cell colonies decreased. High levels of H_2O_2 produced by treatment with MnSOD at an MOI of 200 (>400% ROS compared with control; Figure 1E and F) presumably inhibited E2-induced growth of MCF-7 colonies. To test this postulate, we examined the effect of various concentrations of H_2O_2 on MCF-7 colony formation after 7 days of treatment in the presence or absence of H_2O_2 scavenger (PEG-CAT). Consistent with our postulate, we found that when cells were treated at a low concentration of H_2O_2 (25 μM), the number and size of colonies were increased by more than two-fold compared with controls and these effects of H_2O_2 on MCF-7 colony were prevented by cotreatment with 500 μg ml^{-1} PEG-CAT. Whereas at a high concentration of H_2O_2 (600 μM), both parameters in cell colonies were lower than controls (Figure 1G). This is consistent with reports that lower levels of H_2O_2 support the growth of cells, while higher levels of H_2O_2 are toxic to cells, perhaps by inducing autophagic programmed cell death (Deruy *et al*, 2010). These observations suggest that ROS, particularly H_2O_2 and $O_2^{\bullet -}$, produced by E2 treatment may have an important role in the colony-forming ability of MCF-7 cells.

Cell proliferation and colony formation of E2-treated MCF-7 cells depend on the oxidative state of Trx. The thioredoxin (Trx) system consisting of Trx, NADPH, and Trx reductase (TrxR) functions in thiol-dependent thiol-disulphide exchange reactions, which are crucial in control of the reduced intracellular redox environment. We postulate that these proteins (Trx/TrxR) are responsive to E2-induced ROS in exposed cells and oxidation of these proteins may modulate E2-induced growth of MCF-7 cells. We first determined whether E2-exposed cells showed a change in the redox status of Trx. As expected, we observed higher levels of oxidised Trx after H_2O_2 treatment, while the DTT treatment reduced Trx (Figure 2A). MCF-7 cells treated with E2 (367.1 pM) showed significant oxidation of Trx at 30 min as shown by redox western blot (Figure 2A) and calculated redox potential (EhTrx1)

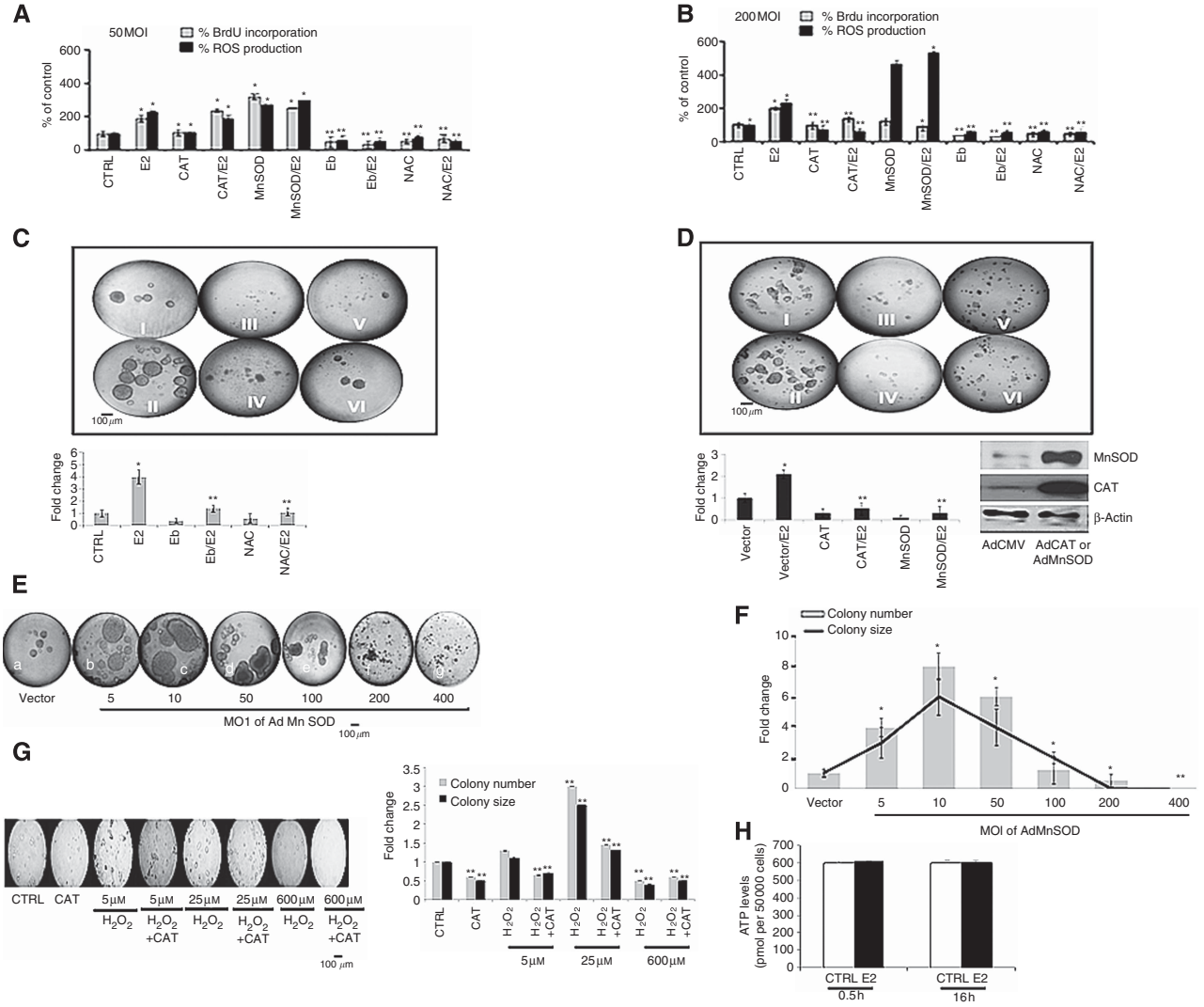

Figure 1. Endogenous ROS regulated E2-induced growth of MCF-7 cells. Production of ROS and bromodeoxyuridine (BrdU) incorporation was determined in MCF-7 cells treated with E2 (367.1 pM) in the presence or absence of ROS modifiers. MCF-7 cells overexpressing manganese superoxide dismutase (MnSOD), catalase (CAT), or pretreated with ROS scavengers ebselen (Eb) (20 μM) or 1 mM of NAC for 4 h were exposed to vehicle (dimethyl sulphoxide (DMSO)) or E2 (367.1 pM) for 30 min before ROS measurements or for 48 h for BrdU incorporation. (**A**) Analysis of ROS by DCF assay and BrdU incorporation assay in MCF-7 cells either transduced with 50 MOI of MnSOD and CAT or pretreated with ROS scavengers. (**B**) Analysis of ROS formation and BrdU incorporation in MCF-7 cells transduced with 200 MOI of MnSOD and CAT or pretreated with ROS scavengers. Values are mean ± s.d. of six independent experiments. (**C**) Effect of ROS scavengers on colony formation in soft agar of E2-treated MCF-7 cells after 21 days. (I) Vehicle control (CTRL), (II) E2, (III) Eb, (IV) Eb + E2, (V) NAC, and (VI) NAC + E2. Bar graph indicates significant inhibition of E2-induced colonies by ROS scavengers. Values for the number of colonies are shown as fold change compared with CTRL. (**D**) Colony assay of E2-treated MCF-7 cells overexpressing MnSOD, CAT, and CTRL vector after 21 days. (I) CTRL vector, (II) vector + E2, (III) CAT, (IV) CAT + E2, (V) MnSOD, and (VI) MnSOD + E2. Bar graph indicates significant inhibition of E2-induced colonies by ROS scavengers. Western blot confirmed overexpression of CAT and MnSOD (MOI = 200) in MCF-7 cells. (**E**) Effect of MnSOD overexpression on MCF-7 colony formation. MCF-7 cells were transduced with various titers of MnSOD (5–400 MOI). (**F**) Bar graph of the effect of MnSOD treatment on MCF-7 colony number and size. Colony efficiency for (**C**, **D**, and **F**) were determined by counting the number of colonies > 65 μm in diameter. Data were expressed as the mean of five wells ± s.d. (**G**) Effect of various concentration of H_2O_2 in the presence or absence of PEG-CAT on MCF-7 colony formation after 7 days of treatment. Bar graph of the effect of H_2O_2 treatment on MCF-7 colony number and size. Values are mean ± s.d. of three independent experiments. (**H**) ATP levels present in the MCF-7 cells exposed to vehicle (DMSO) or E2 (367.1 pM) for 0.5 and 16 h. ATP levels in the cells were measured by recording the luminescence of CellTiter-Glo Reagent (Promega). *P < 0.05, significant difference from that of CTRL. **P < 0.05, significant difference from E2 or H_2O_2 treatment.

measurements (Figure 2B). Erucin has been shown to be a potent inducer of TrxR in MCF-7 cells (Wang *et al*, 2005a); therefore, we examined the effects of erucin on E2-induced oxidation of Trx. As shown in Figure 2A, pretreatment with erucin suppressed the level of oxidised Trx, presumably through an increase in Trx reductase levels that were able to handle the increased level of E2-induced ROS. These experiments show that the oxidation of Trx occurs by E2 treatment and redox potential of MCF-7 cells is shifted towards a reduced environment. After confirming that E2 treatment oxidised Trx in MCF-7 cells, we determined the effects of Trx modifier erucin on E2-induced cell proliferation and colony formation in MCF-7 cells. We observed that the dose of erucin (10 μM) already reported induce the expression of TrxR (Wang *et al*, 2005a) significantly decreased BrdU incorporation and

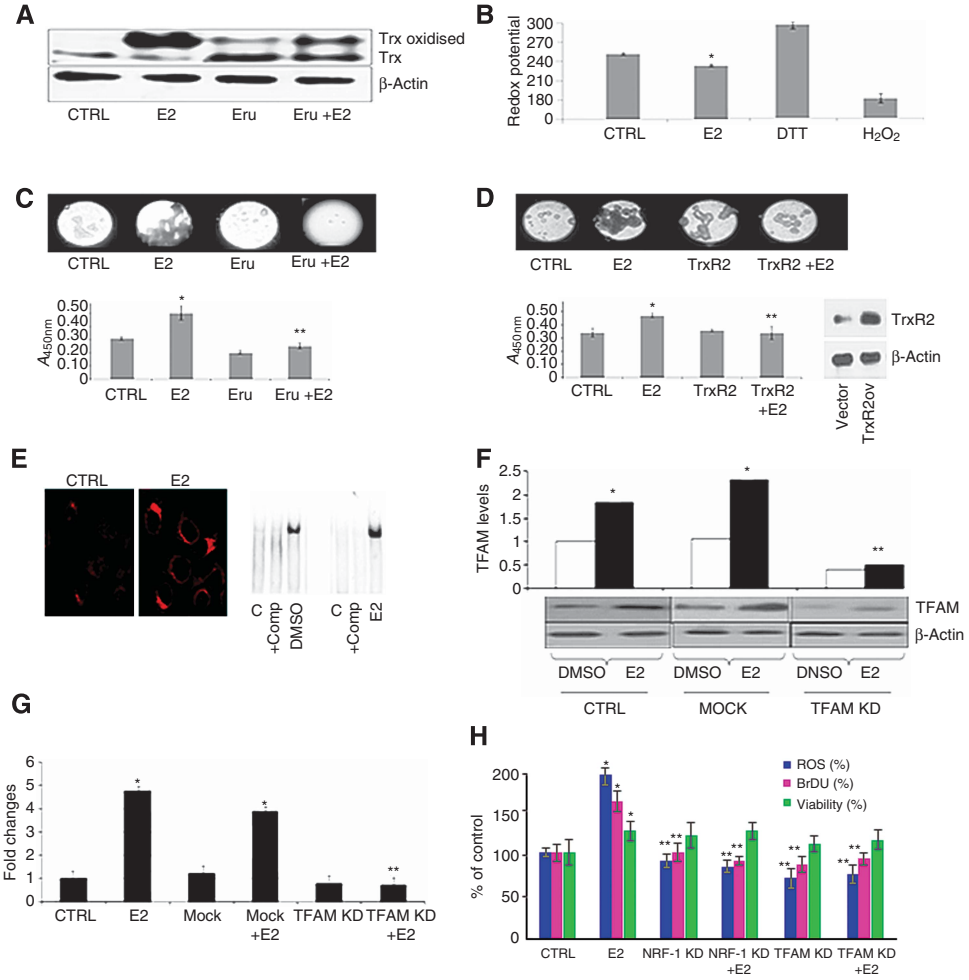

Figure 2. Cell proliferation and colony formation of E2-treated MCF-7 cells depend on the oxidative state of Trx and mitochondrial biogenesis genes. Changes in the oxidation state of Trx associated with impaired E2-induced colony formation. (**A**) Comparison of Trx oxidation in MCF-7 cells treated for 30 min with E2 (367.1 pM) or the chemical inducer of TrxR erucin (Eru) by redox western blot analysis. 17β-Oestradiol treatment showed a higher level of oxidised Trx (top band) compared with vehicle (dimethyl sulfoxide (DMSO)) and reduced the level of oxidised Trx in a 48 h pre-treatment with 10 μM Eru. (**B**) Values in the graph are of the steady-state redox potential (Eh) for Trx oxidation in MCF-7 cells treated with reductant (dithiothreitol (DTT), 5 mM), oxidant (H_2O_2, 2 mM), and E2. (**C**) Comparison of colony formation in soft agar at 14 days of E2-treated MCF-7 cells when cotreated with Eru. Values in the graph show significant inhibition of E2-induced bromodeoxyuridine (BrdU) incorporation by Eru treatment. (**D**) Comparison of colony formation in E2-treated MCF-7 cells with and without overexpression of TrxR2 for 48 h. Graph indicates significant inhibition of E2-induced BrdU incorporation when MCF-7 cells overexpress TrxR2. Western blot confirmed overexpression of TrxR2. (**E**) Analysis of E2 effects on mitochondrial mass with MitoTracker Red. MCF-7 cells showed increased mitochondrial labelling intensity in E2 treatment compared with control (CTRL). Comparison of E2-induced NRF1 DNA-binding activity by EMSA showed increased NRF1 binding at 3 h. C = CTRL; + Comp = negative NRF1-binding CTRL. (**F**) Comparison of cellular protein levels of TFAM in short hairpin RNA (shRNA) Tet-off/on cells. Western blot confirmed lower protein level of TFAM by inducible shRNA in MCF-7 cells. Values are shown in the graph of protein band intensity as well as in the immunoblot of TFAM Tet/on cells (TFAM knockdown (KD)) compared with Tet/off cells (Mock). (**G**) Comparison of E2-induced MCF-7 colony formation in TFAM Tet/on cells (TFAM KD) compared with Tet/off cells (Mock). (**H**) Comparison of NRF-1 and TFAM KD effects on ROS formation, BrdU incorporation, and cell viability in E2-treated MCF-7 cells. Values are mean ± s.d. Data shown in each panel are representative of three independent experiments. *$P<0.05$, significantly different from CTRL. **$P<0.05$, significantly different from E2.

colony formation in both control- and E2-treated MCF-7 cells (Figure 2C). Next, we confirmed these results by directly overexpressing the enzyme TrxR2. As expected, we observed that the overexpression of TrxR2 (confirmed by western blot) decreased the proliferation and colony formation of E2-treated MCF-7 cells when compared with vehicle control (Figure 2D). Taken together, these findings support a role of the Trx system in controlling E2-induced growth of MCF-7 cells.

Role of mitochondria in regulating ROS production and prevention of E2-induced MCF-7 colony formation. Previously, we have reported that E2-induced growth of MCF-7 cells depend in part on ROS of mitochondrial origin (Felty *et al*, 2005a). Mitochondria are highly dynamic organelles, frequently dividing and fusing in response to physiological and environmental conditions. To further establish that the growth of MCF-7 cancer cells is mediated by ROS produced by mitochondria, we examined the effect of inhibition of genes responsible for mitochondrial biogenesis. The effect of E2 treatment on mitochondrial mass was examined by confocal microscopy. The fluorescent probe Mito-Tracker Red was used to label mitochondria and its fluorescent intensity served as a surrogate for mitochondrial mass. As shown in Figure 2E, E2 treatment (367.1 pM) increased MitoTracker Red 580 labelling, indicating E2 treatment increased MCF-7

cells mitochondrial mass (Figure 2E). Mitochondrial transcription factor A controls mitochondrial biogenesis (Okoh *et al*, 2011). Mitochondrial transcription factor A is known to regulate not only mitochondrial biogenesis but also mtDNA stability and the biosynthesis of the 13 mtDNA-encoded respiratory chain subunits. As E2 treatment showed an increase in the mitochondrial mass, we postulated that E2 increased the DNA-binding activity of NRF1, a regulator of TFAM as well as the level of TFAM. Using EMSA, we observed a several fold increase in NRF1 DNA-binding activity as early as 3 h (Figure 2E) in treated MCF-7 cells. As shown in Figure 2F, E2 treatment (367.1 pM for 24 h) resulted in a two-fold increase in total TFAM protein that was inhibited by treatment with inducible TFAM shRNA system. Western blot analysis confirmed inhibition of the levels of TFAM protein by shRNA treatment. Inducible TFAM shRNA inhibited MCF-7 colony formation in E2-treated cells (Figure 2G). We also determined whether the observed reduction in MCF-7 colonies was due to cell death from TFAM knockdown. The percentage of viable cells in both treatment groups for TFAM shRNA was very similar to control cells (Figure 2H). Furthermore, knockdown of TFAM resulted in the inhibition of E2-induced ROS that was to be expected because we have already showed that mitochondria are a major source of ROS in E2-treated MCF-7 cells. DNA synthesis was inhibited in E2-exposed MCF-7 cells by the silencing of TFAM (Figure 2H), which is corroborated by our previous study that showed MCF-7 ρ^0 cells had decreased E2-induced DNA synthesis because of impaired mitochondrial biogenesis (Felty *et al,* 2005b). To discern whether a decrease in ATP production or ROS may be responsible for the E2-induced growth signalling, we measured the ATP present in the MCF-7 cells exposed to vehicle (DMSO) or E2 (367.1 pM) for 0.5 and 16 h (Figure 1H). Our data showed that the ATP levels in both treatment groups for E2 were very similar to control cells. This is consistent with our previous studies in MCF-7 cells, indicating that modulation of mitochondrial function, mitochondrial protein synthesis, or mitochondrial transcription/replication block E2-induced cell cycle progression from G1 to S phase without influencing the level of ATP (Felty *et al*, 2005b). Taken together, these data suggest that mitochondria are a source of E2-induced ROS, which in part contribute to the growth of MCF-7 cells.

Oxidation of PTPs and ROS-induced phosphorylation of ERK and AKT in E2-treated MCF-7 cells may be responsible for the growth of breast cancer cells. Here the aim was to identify the cell signalling mechanism contributing to the growth of malignant breast cancer cells. We previously showed that E2-induced DNA synthesis in MCF-7 breast cancer cells depends, in part, on ROS-mediated signalling to nuclear transcription factors, including NRF-1 (Felty *et al*, 2005a). The question that remains unanswered is how E2-induced ROS transduce a signal to nuclear regulatory proteins that participate in breast cancer cell growth. We postulated that the transient inhibition of protein tyrosine phosphatases (PTPs) through the reversible oxidisation of their catalytic cysteine ultimately suppresses protein dephosphorylation of PTP-interacting proteins. Furthermore, we postulated that this redox-sensitive pathway is coupled to the activation of downstream nuclear regulatory proteins in response to E2-induced ROS signalling. Therefore, we investigated the effects of E2-mediated redox regulation of PTPs (PTEN and CDC25A) and their downstream effects on PTP-regulated proteins (ERK and AKT) that ultimately signal nuclear regulatory proteins (NRF-1, ERα and p27) in MCF-7 cells.

Endogenous ROS regulated E2-induced oxidation of PTEN and CDC25A. Signal transduction by ROS through reversible PTP inhibition may be a major mechanism used by E2-dependent breast cancer cells. 17β-Oestradiol treatment has been shown to cause a significant decrease of PTEN activity (Marino *et al*, 2003). Reactive oxygen species such as H_2O_2 and superoxide also decrease PTEN activity through the oxidation of PTEN's cysteine residues (Lee *et al*, 2002). Therefore, we measured whether the inhibition of PTEN by E2 is mediated by ROS. First, we confirmed whether H_2O_2, known to oxidise PTPs, could oxidise PTEN in MCF-7 cells (Lee *et al*, 2002). As shown in Figure 3A, 0.2 mM H_2O_2 did not induce PTEN oxidation and treatment with reductant DTT showed only reduced form of PTEN. There was no difference in PTEN oxidation in untreated MCF-7 cells and 0.2 mM H_2O_2-treated MCF-7 cells (data not shown). Treatment of MCF-7 cells with higher doses of H_2O_2 (0.5–1.0 mM) produced very pronounced oxidised form of PTEN compared with that of 0.2 mM H_2O_2-treated MCF-7 cells. As we showed previously, treatment with TAM and E2 increased the level of ROS in MCF-7 cells. Therefore, we first determined the oxidation of PTEN in E2-treated MCF-7 cells. Our results showed that E2 treatment increased PTEN oxidation (Figure 3B), which was inhibited by cotreatment with the ROS scavenger ebselen.

We also tested the effects of E2-induced ROS on CDC25A because it contains a highly reactive cysteine at the active site that can react directly with ROS, leading to enzyme inactivation and thus may be another potential redox-sensitive PTP. The oxidation of CDC25A was determined in MCF-7 cells treated with E2 or H_2O_2. MCF-7 cells showed increased oxidative modification (decreased 5-IAF labelling) of CDC25A to E2 (Figure 3C) as well as a parallel decrease in phosphatase activity in response to E2 and H_2O_2 (Figure 3D). Furthermore, we determined the effects of E2 and H_2O_2 on serine phosphorylation of CDC25A (Figure 3E). Cotreatment with ROS scavenger NAC not only counteracted E2-induced oxidative modification of CDC25A, which was shown by increased 5-IAF labelling in NAC + E2 group compared with E2 alone (Figure 3C), but also prevented the decrease in CDC25A phosphatase activity from E2 treatment (Figure 3D) that was supported by an associated decrease in phosphorylation (Figure 3E). In contrast to serine phosphorylation of CDC25A, we observed an increase in tyrosine phosphorylation in cells treated with E2 or H_2O_2 (Figure 3F) and this was inhibited by cotreatment with NAC. To rule out whether a decrease in CDC25A activity under conditions of E2-induced ROS was not because of the degradation of CDC25A protein, we analysed CDC25A levels in the presence and absence of the ROS scavenger NAC. As shown in Figure 3G, we observed an increase in the level of CDC25A protein as early as 3 h after E2 exposure. Cotreatment with ROS scavenger NAC or mitochondrial complex I inhibitor rotenone, which was known to block mitochondrial oxidant generation, showed a decrease in E2-induced CDC25A protein compared with control. These findings suggest that the decrease in CDC25A phosphatase activity by E2 treatment was not because of the degradation of CDC25A, but rather these data support the idea that E2-induced ROS may inhibit phosphatase activity, presumably by oxidation of the Cys-SH residue perhaps by modulating serine phosphorylation of CDC25A.

Endogenous ROS regulated E2-induced ERK and AKT phosphorylation. Both ERK and AKT are important kinases regulated by E2 and are downstream components of a signalling pathway involving PTPs CDC25A and PTEN. Phospho-ERK has been shown to be a substrate of CDC25A (Wang *et al,* 2005). Therefore, we determined whether treatment with ROS scavengers decreased E2-induced phosphorylation of ERK. As shown in Figure 3H, a 30 min treatment of MCF-7 cells with E2 (367.1 pM) increased the levels of phosphorylated ERK. This is in agreement with previous studies (Migliaccio *et al*, 1996; Marino *et al*, 2003). Next, we determined whether E2-induced increase in p-ERK depended on ROS. As shown in Figure 3H, overexpression of CAT and MnSOD inhibited the phosphorylation of ERK in E2-treated MCF-7 cells, but did not affect

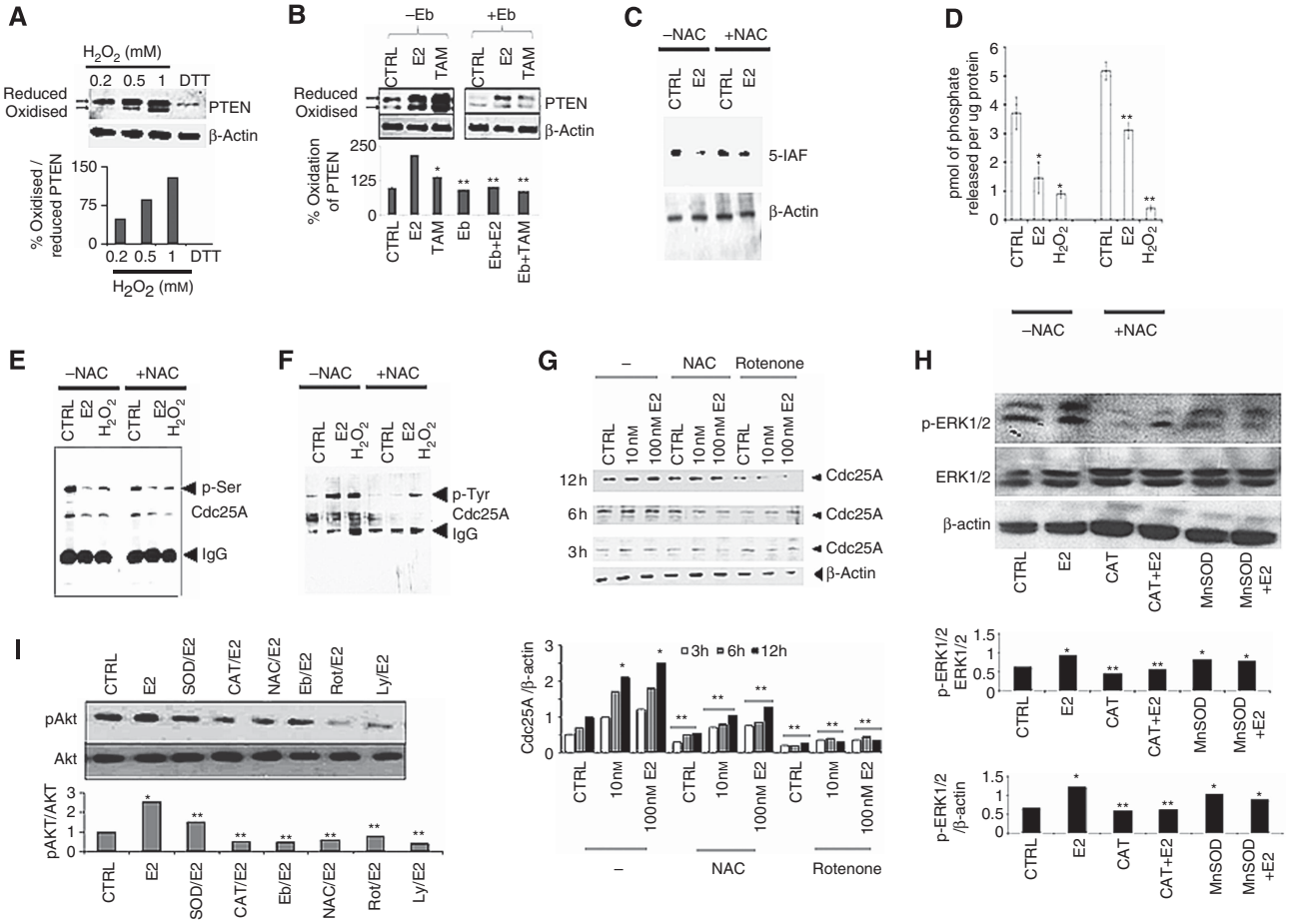

Figure 3. Oxidation of PTPs and ROS-induced phosphorylation of ERK and AKT in E2-treated MCF-7 cells. Changes in the oxidation state of PTPs, PTEN, and CDC25A were determined by western blot analysis. (**A**) Comparison of PTEN oxidation in MCF-7 cells treated with oxidant H_2O_2 and reductant dithiothreitol (DTT) (5 mM) for 30 min. Higher doses of H_2O_2 (0.5 and 1.0 mM) showed higher levels of oxidised PTEN (bottom band) compared with 0.2 mM dose of H_2O_2 and DTT. (**B**) Comparison of PTEN oxidation in E2-treated MCF-7 cells when pretreated with 20 μM of ROS scavenger ebselen (Eb) for 4 h. Western blot showed increased PTEN oxidation by both E2 (367 nM) and 1 μM tamoxifen (TAM) treatment in MCF-7 cells compared with control (CTRL) (dimethyl sulfoxide (DMSO)) and this was suppressed by Eb. Values in graph represent % oxidised/reduced PTEN from three independent experiments ± s.d. (**C**) Comparison of CDC25A sulphydryl labelling by 5-iodoacetamidofluorescein (5-IAF) reagent in MCF-7 cells treated with E2 (10 ng ml^{-1}) for 30 min in the presence or absence of 10 mM of ROS scavenger NAC. Decreased 5-IAF labelling indicated a decrease in free sulphydryl (− SH) groups present in CDC25A. (**D**) Analysis of CDC25A phosphatase activity in MCF-7 cells treated with E2 and H_2O_2 as described previously. Values in the graph represent CDC25A phosphatase activity from IP lysate of MCF-7 cells treated with NAC. Enzyme activity was tested *in vitro* using OMFP as a substrate. (**E**) Comparison of CDC25A serine phosphorylation in E2- and H_2O_2-treated MCF-7 cells when pretreated with NAC as described previously. (**F**) Comparison of CDC25A tyrosine phosphorylation in E2- and H_2O_2-treated MCF-7 cells when pretreated with NAC as described previously. Cell lysates were IP with CDC25A antibody and immunoblots were detected for anti-phosphotyrosine (p-Tyr) or -serine (p-Ser). IgG bands served as a loading CTRL ($n = 2$). (**G**) Western blot analysis of the effects of NAC (10 mM) and mitochondrial ROS blocker rotenone (Rot) (5 μM) on CDC25A protein levels in E2-treated MCF-7 cells. (**H**) Western blot analysis of the effects of MnSOD and CAT (MOI = 200) overexpression on E2 (367 pM)-induced ERK phosphorylation in MCF-7 cells. Values in the graph represent a ratio of levels of phospho-ERK1/2 compared with total ERK1/2 or β-actin from three independent experiments. (**I**) Western blot analysis of the effect of ROS modifiers on E2-induced AKT phosphorylation in MCF-7 cells. Experimental conditions are the same as described previously. Treatment with 10 μM of PI3K/AKT pathway inhibitor LY294002 (Ly) served as a positive CTRL of p-AKT inhibition. Values in the graph are the densitometry data of p-AKT normalised to total AKT expressed as fold change compared with CTRL. The quantitative values are mean ± s.d. Data shown in this figure are representative of three independent experiments. *$P < 0.05$, significant difference from CTRL. **$P < 0.05$, significant difference from E2. SOD, superoxide dismutase.

ERK protein expression (Figure 3H). The data suggest that ERK1/2 activation is a downstream effector of E2-induced ROS. Given the previous observations that CDC25A interacted with ERK and CDC25A was oxidised in E2-treated MCF-7 cells, the subsequent inhibition of CDC25A phosphatase activity may allow for the continued phosphorylation of ERK (Wang *et al*, 2005).

As PTEN through the phosphoinositol 3′ kinase (PI3K) pathway is known to regulate AKT, we also determined the effect of ROS modifiers on phosphorylation of AKT in E2-treated MCF-7 cells. As expected, treatment of MCF-7 cells increased phosphorylation of AKT (Figure 3I). 17β-Oestradiol -induced phosphorylation of AKT was reduced by either overexpression of antioxidant enzymes CAT or MnSOD and ROS scavengers ebselen or NAC. There was no difference in the phosphorylation of AKT in vehicle- and NAC-, rotenone-, or ebselen-treated cells (background levels, data not shown). Therefore, we have used the same controls as a representation for both vehicle- and NAC-, rotenone-, or ebselen-treated control experiments. Studies of the mitochondrial electron

transport chain have reported ROS-forming sites at the FMN group of complex I (Turrens *et al* 1985). Therefore, we used a specific chemical blocker of mitochondrial respiratory complex I (rotenone) to determine whether phosphorylation of AKT depended on mitochondrial ROS. As shown in Figure 3I, mitochondrial complex I inhibitor rotenone showed a significant inhibition of E2-induced AKT phosphorylation. The known chemical inhibitor of PI3K, which regulates AKT activation, LY294002, was used as a positive control and confirmed that E2 increased the level of p-AKT in MCF-7 cells (Figure 3I). These data support that E2-induced ROS signalling occurs upstream of AKT and E2-induced ROS inactivation of PTEN may allow the increased phosphorylation of the known downstream kinase AKT. Taken together, these findings suggest that ERK or AKT individually or in concert are susceptible to E2-induced ROS-mediated phosphorylation.

Endogenous ROS regulated AKT-mediated phosphorylation of NRF-1. To further investigate the mechanism by which the redox regulation of AKT by E2-induced ROS controls growth of MCF-7 cells, we examined the effects of E2 on the redox-sensitive transcription factor NRF-1 (known to control mitochondrial biogenesis as well as the fate of cells) in the presence or absence of ROS or AKT modifiers. First, we evaluated whether the oxidant-dependent phosphorylation of NRF-1 is a function of AKT-dependent signalling by *in vitro* kinase assays using recombinant human NRF-1 and active recombinant human AKT. Serine-phosphorylated wild-type NRF-1 was detected only in the presence of AKT (Figure 4A). Next, we used mass spectrometry to identify the specific serine or threonine site(s) and tyrosine phosphorylation sites on NRF-1 that was phosphorylated by the kinase. The MS/MS spectrum for the NRF-1 peptide containing phospho-threonine at residue 109 (observed mass of peptide sequence 106–114 ATLDEYTTR is shown in Figure 4B). This site has been previously reported to be phosphorylated by AKT in murine cells (Piantadosi and Suliman, 2006). Our data also showed that tyrosine residues 215 (Y215) and 326 (Y326) were phosphorylated by recombinant kinase AKT (data not shown). Two other novel serine residues at 91 (observed mass of peptide sequence 82–93 RPHVFESNPSIR) and at 127 (observed mass of peptide sequence 115–134 VGQQAIVL-CISPSKPNPVFK), which is theoretically predicted to be a consensus acetylating site (SPSKP), are also targeted by AKT (data not shown). Phosphorylation on serines 39, 44, 46, and 48 targeted by CKII (Herzig *et al*, 2000) and serine 51 targeted by cyclin D1 (Wang *et al*, 2006) was not detected by mass spectrometry.

To provide further evidence supporting the *in vitro* kinase assay observation that AKT phosphorylates NRF-1, we conducted co-IP experiments to determine whether E2 treatment increased NRF-1/AKT protein–protein interactions. As shown in Figure 4C, endogenous NRF-1 co-IP with AKT and this interaction was increased by E2 exposure (367.1 pM for 30 min) of MCF-7 cells. This protein–protein interaction was determined to be specific because the NRF-1-containing lysates were not IP with non-immune rabbit serum (data not shown). To confirm that AKT controls NRF-1 phosphorylation, we examined the effect of shRNA-mediated AKT1 knockdown on NRF-1 phosphorylation. As shown in Figure 4D–F, cells transfected with AKT1 shRNA had a lower level of AKT1 in MCF-7 cells. We observed that phosphorylation of NRF-1 was markedly lower upon E2 treatment in AKT1 shRNA cells compared with cells transfected with non-targeting control scrambled shRNA cells, while NRF-1 protein levels were not affected by AKT1 silencing in MCF-7 cells. (Figure 4D–F). Taken together, these data implicate that NRF-1 is a physiological substrate of AKT1. Using AKT1 shRNA, we also confirmed whether silencing the suspected upstream kinase responsible for phosphorylation of NRF-1 in E2-treated MCF-7 cells would have an inhibitory effect on colony formation. As expected, cells that were transfected with AKT1 shRNA showed a much lower frequency of colonies after E2 treatment compared with the cells transfected with non-targeting control shRNA (Figure 4G).

Based on our previous findings that show that NRF-1 is a substrate of the kinase AKT, we determined whether NRF-1 phosphorylation was increased in MCF-7 cells. As shown in Figure 4H, we observed more than a two-fold increase in phospho-NRF-1 in E2-treated (367.1 pM for 30 min) MCF-7 cells. To confirm our results from western blots, we used immunofluorescence microscopy to evaluate NRF-1 phosphorylation. As shown in Figure 4I, colocalisation of two antibodies (anti-phosphoserine and anti-NRF-1) was used to measure the level of phospho-NRF-1. Phosphorylated serine was captured as blue, and NRF-1 was captured as red. Colocalisation of phosphorylated serine and NRF-1 yielded pink staining, which served as an indicator of phospho-NRF-1. Phospho-NRF-1 colocalised mainly in the nuclei after E2 treatment (Figure 4I). As shown in Figure 4H and J, phosphorylation of NRF-1 was inhibited by cotreatment with either biological (CAT or MnSOD) or chemical (20 μM ebselen) ROS modifiers. These results suggest that E2-induced phosphorylation of NRF-1 is influenced by ROS signalling messengers.

Silencing of NRF-1 and AKT inhibited E2-induced MCF-7 colony formation. Next, we evaluated whether NRF-1 or AKT expression was required for E2-induced stimulation of anchorage-independent growth. We altered the levels of these proteins by their respective shRNA targeting their mRNAs in MCF-7 cells and examined whether silencing of NRF-1 or AKT1 was able to inhibit E2-induced *colony* formation. As shown in Figure 4K, shRNA targeting NRF-1 inhibited the expression of both NRF-1 and phospho-NRF-1 proteins in MCF-7 cells. As expected, the shRNA silencing of NRF-1 led to the downregulation of *TFAM*, an NRF-1 target gene (Figure 4K). In addition, knockdown of NRF-1 resulted in the inhibition of anchorage-independent growth of MCF-7 cells in both vehicle control- and E2-treated cells (Figure 4L). Furthermore, we determined whether the observed reduction in colonies was due to cell death from NRF-1 knockdown. The percent of viable cells in NRF-1 knockdown were very similar to control cells (Figure 2H). Furthermore, knockdown of NRF-1 resulted in the inhibition of E2-induced ROS, which was to be expected as we have already shown that mitochondria are the major source of ROS in MCF-7-exposed cells. We also observed an inhibition of DNA synthesis in E2-exposed MCF-7 cells by the RNA interference (RNAi) silencing of NRF-1.Taken together, these findings support the idea that NRF-1 may have an important role in E2-induced growth of MCF-7 cells.

Endogenous ROS production regulated E2-induced NRF-1-dependent transcriptional activation of cell cycle genes. Based on our data that showed inhibited E2-induced DNA synthesis by silencing NRF-1 mRNA expression in MCF-7 cells, we postulated that E2-induced ROS signalling is involved in the modulation of NRF-1-dependent cell cycle genes. Our next investigations used a ChIP promoter assay to determine whether ROS modifiers altered NRF-1 binding to the promoters of cell cycle genes that are known to be regulated by this transcription factor. As shown in Figure 5A and B, we observed NRF-1 bound to the promoters of CDC2, PRC1, PCNA, cyclin B1, and CDC25C and confirmed that these promoters contain NRF-1 elements. We also found that E2-treated MCF-7 cells showed increased NRF-1 binding to the promoters of these genes. NRF-1 binding induced by E2 treatment was inhibited by the overexpression of CAT and MnSOD. Next, we determined whether an increase in cell cycle gene expression occurred as a result of ROS-dependent NRF-1 binding to the respective promoters of these genes. We observed a significant increase in the mRNA expression of CDC2, PRC1, PCNA, cyclin B1, and

CDC25C (Figure 5C). Overexpression of MnSOD or CAT inhibited E2-induced expression of CDC2, PRC1, PCNA, cyclin B1 and CDC25C when compared with E2 treatment alone. These results suggest that E2-generated ROS signal NRF-1 binding to the promoter of cell cycle genes and thus control the expression of these cell cycle genes.

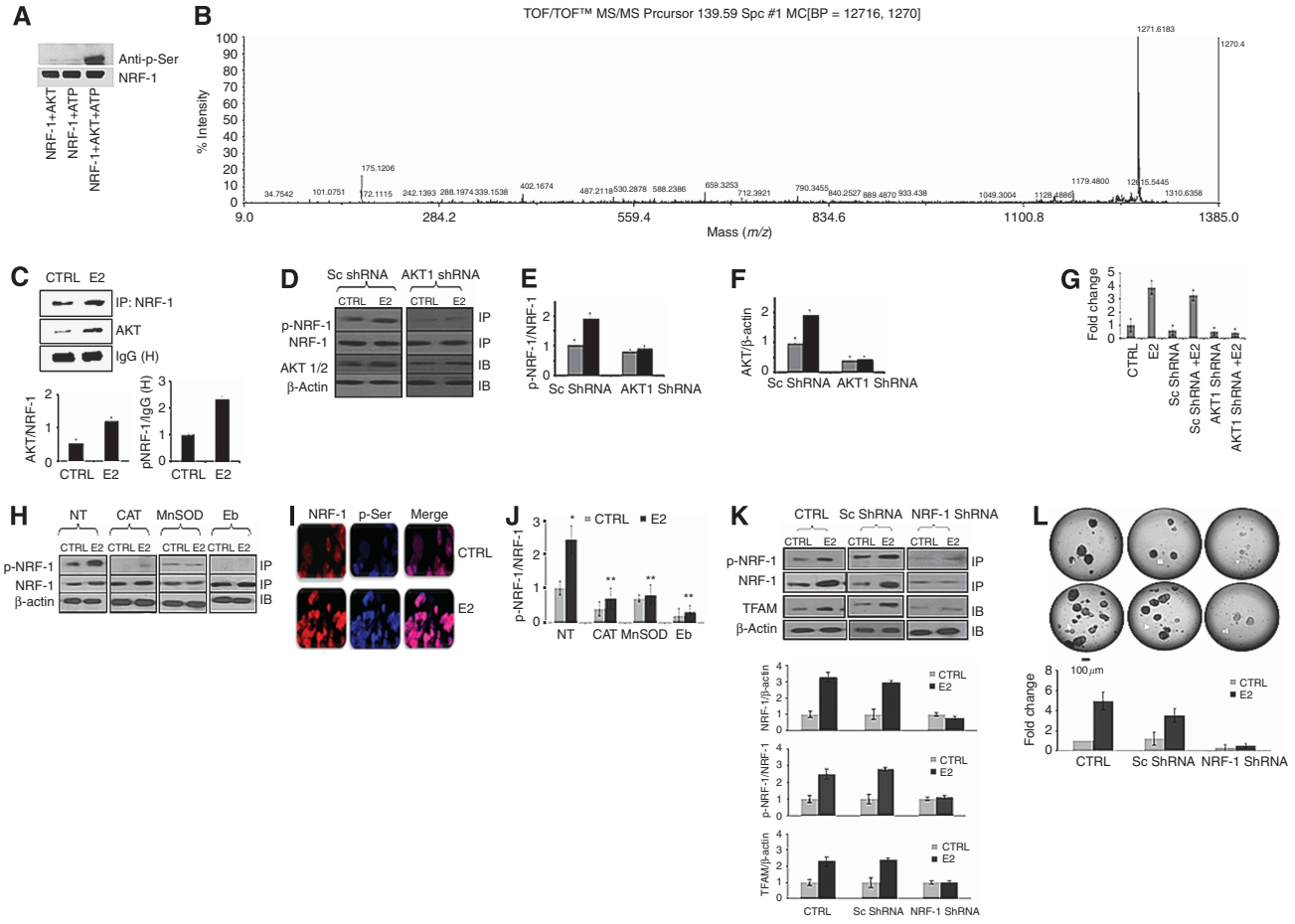

Figure 4. AKT-mediated phosphorylation of NRF-1 and NRF-1-dependent E2-induced MCF-7 colony formation. (**A**) Analysis of NRF-1 phosphorylation by *in vitro* AKT kinase assay. Recombinant AKT kinase was incubated with NRF-1 in the presence or absence of ATP, and serine phosphorylation was detected by immunoblot (IB). (**B**) *In vitro* phospho-NRF-1 was confirmed by combined MS + MS/MS as described previously. The presence of phosphorylated amino acids was identified by the MS/MS peak showing the neutral loss of phosphates for the NRF-1 peptide containing phosphothreonine at residue 109 of the peptide with observed mass of phospho-(S/T) with sequence 106–114 ATLDEYTTR. The x axis represents mass and y axis represents intensity. (**C**) Analysis of AKT/NRF-1 protein–protein interaction in 30 min E2- (367 pM) treated MCF-7 cells. Total cell lysates were IP with anti-NRF-1 antibodies and proteins were detected by IB with anti-NRF-1 and anti-AKT antibodies. Densitometry measurements represented as a ratio of AKT normalised to NRF-1 or IgG. (**D**) Analysis of the effect of AKT short hairpin RNA (shRNA) treatment on E2-induced phosphorylation of NRF-1 in MCF-7 cells. Cells were transfected with AKT shRNA or scrambled (Sc) control for 48 h. IBs detected the effect of AKT shRNA on total levels of AKT and NRF-1. Cell lysates IP with anti-NRF-1 antibody were used to determine NRF-1 phosphorylation with anti-phosphoserine antibodies. (**E**) Values in the graph represent densitometry measurements of previously described experiment. The band intensity for anti-phosphoserine corresponded to the MW 65 kDa for NRF-1 (denoted as pNRF-1) was normalised to total NRF-1. (**F**) Values in the graph represent densitometry measurements of AKT normalised to β-actin and confirm inhibition of AKT by shRNA. Data shown (**E** and **F**) are representative of three independent experiments ± s.d. (**G**). Comparison of the effect of AKT shRNA treatment on E2-induced MCF-7 colonies grown in soft agar for 21 days. Graph shows significant reduction in the number of E2-induced colonies by inhibition of Akt expression. Values for the number of colonies shown as fold change compared with control. (**H**) Comparison of E2-induced phosphorylation of NRF-1 at 4 h in MCF-7 cells overexpressing MnSOD and CAT (MOI = 200) or treated with 20 μM ebselen (Eb) determined by western blot. (**I**) Confirmation of *in vivo* phosphorylation of NRF-1 in E2- (367 pM) treated MCF-7 cells at 30 min. Colocalisation of Alexa Fluor 488 mouse anti-phosphoserine (in blue) and Alexa Fluor 633 rabbit anti-NRF-1 (in red) antibodies were used as a marker of phospho-NRF-1 shown in merged photo. (**J**) Values in the graph represent densitometry measurements of previously described experiment. The band intensity for anti-phosphoserine corresponded to the MW 65 kDa for NRF-1 denoted as pNRF-1 was normalised to total NRF-1. (**K**) IB analysis of the effect of NRF-1 shRNA treatment on E2 (367 pM) - induced phosphorylation of NRF-1 and expression of its target gene *TFAM* in MCF-7 cells. IBs were probed for anti-phosphoserine corresponded to the MW 65 kDa for NRF-1, total NRF-1, TFAM, and β-actin as a loading control. Values in the graph represent densitometry measurements of previously described experiment. Reduction in *TFAM* normalised to β-actin confirmed significant inhibition of this target gene by NRF-1 shRNA. (**L**) Comparison of the effect of NRF-1 shRNA treatment on E2-induced MCF-7 colony formation after 21 days. Upper panel graph indicates CTRL wild-type, E2 wild-type, and CTRL shRNA. Middle panel graph indicates CTRL shRNA + E2, NRF-1 shRNA, and NRF-1 shRNA + E2. Lower panel graph indicates significant reduction in the number of E2-induced colonies by inhibition of NRF-1 expression. Values for the number of colonies shown as fold change compared with control. Values represent mean ± s.d. Data shown in each panel of this figure are representative of three independent experiments, unless otherwise indicated. *$P<0.05$, significant difference from control. **$P<0.05$, significant difference from E2.

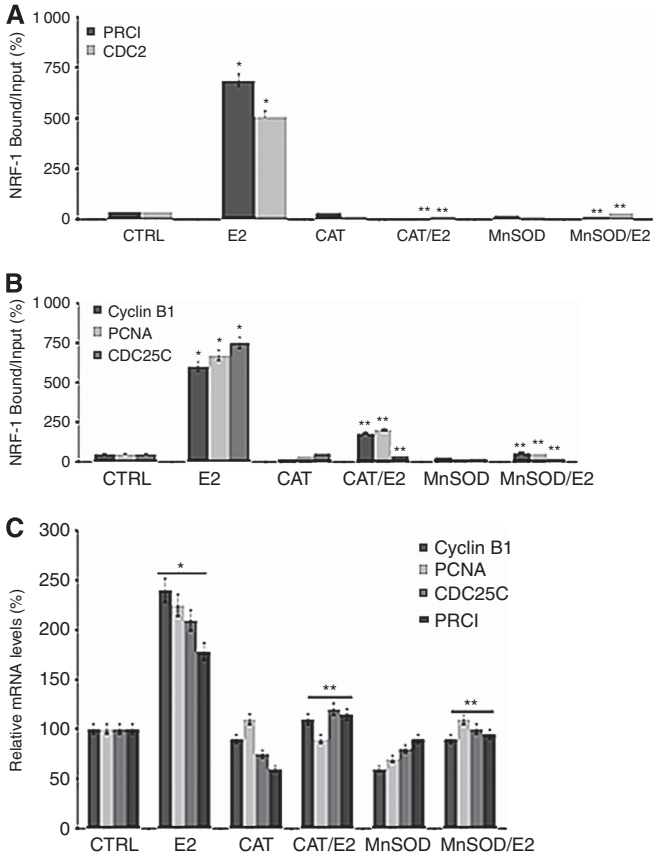

Figure 5. Endogenous ROS regulate NRF-1-dependent transcription of cell cycle genes in E2-treated MCF-7 cells. Chromatin immunoprecipitation quantitative PCR (qPCR) analysis was used to determine NRF-1 binding to the promoters of cell cycle genes when MCF-7 cells were treated with E2 (367 nM) for 16 h. (**A**) Analysis of E2-induced NRF-1 binding to promoters of PRC1 and CDC2. Graph indicates significant reduction in bound NRF-1 to target gene promoters when cells overexpressed ROS-scavenging enzymes manganese superoxide dismutase (MnSOD) and catalase (CAT). (**B**) Analysis of E2-induced NRF-1 binding to promoters of cyclin B1, PCNA, and CDC25C. Graph indicates significant reduction in bound NRF-1 to target gene promoters when cells overexpressed MnSOD and CAT. Each ChIP value that measures bound NRF-1 to target promoter is represented as a percentage of the respective input DNA (NRF-1 bound/input (%)). All ChIP data represent the mean ± s.d. from three independent experiments. *A statistically significant difference from control (CTRL); **a statistically significant difference from E2 treatment. (**C**) Analysis of E2-induced mRNA expression of previously described cell cycle genes. Graph indicates significant reduction in E2-induced gene expression when cells overexpressed enzymes CAT and MnSOD. The relative mRNA levels measured for each gene were normalised to 18S RNA. The expression in the CTRL was set as 100%. Values are mean ± s.d. of three independent experiments. *$P<0.05$, significantly different from CTRL. **$P<0.05$, significantly different from E2.

Endogenous ROS regulated antioestrogen signalling. Although the primary mechanism of the E2 antagonist TAM is considered to work through its inhibition of ER activation, research over the years has indicated that additional non-ER-mediated mechanisms exist. The prevention of breast cancer cell growth by blocking ER signalling with chemicals such as TAM does not necessarily mean that this compound inhibits cancer only through the competitive binding of the receptor. As TAM can block the metabolism/redox cycling of E2 as well as act like free radical scavengers (Arteaga *et al*, 2003), it is possible that the therapeutic effect of this chemical in part occurs through the inhibition of endogenous ROS signals to nuclear regulatory proteins. Therefore, we also investigated the ability of MCF-7 cells to produce ROS in response to exposure with TAM at a pharmacological concentration of 1 μM. Using immunofluorescence microscopy, we observed an increase of intracellular DCFH intensity in MCF-7 cells exposed for 30 min to TAM (shown in green in Figure 6A). Cell mitochondria were also labelled by MitoTracker Red and the merged yellow colour represents ROS formation specific to mitochondria compared with the vehicle control cells. Our results that show TAM indeed increased the intracellular level of ROS is corroborated by another study of TAM-induced ROS in MCF-7 cells (Kallio *et al*, 2005). The ability of TAM to produce ROS was inhibited by treatment with PEG-CAT (500 μg ml^{-1}) and ebselen (20 μM) (Figure 6B). We also measured the effect of TAM treatment on the oxidation of PTEN. We found that TAM treatment increased PTEN oxidation (Figure 3B) and the oxidation of PTEN by these treatments was suppressed by cotreatment with the ROS scavenger ebselen. These results suggest that TAM-induced ROS oxidised PTEN, which is capable of catalytic inactivation of PTEN and may result in the increased phosphorylation of the known downstream kinase AKT.

AKT has been shown to phosphorylate ERα (Marino *et al*, 2003). As ROS is known to activate AKT, we investigated the contribution of ROS to the phosphorylation of ER in E2-treated MCF-7 cells. 17β-Oestradiol-induced phosphorylation of ERα in the presence or absence of ROS modifiers was investigated by is dependent on intracellular ROS production. Comparison of the effect of ebselen on the phosphorylation of ERα was determined by immunofluorescent microscopy. The intensity of phosphorylated ERα at serine was remarkably high in the E2 treatment group (367 pM for 30 min) compared with the vehicle control (Figure 6C and D). Cotreatment of E2 with the ebselen (20 μM), a potent scavenger of H_2O_2, hydroperoxides, and peroxynitrite, decreased E2-induced phosphorylation of ERα in MCF-7 cells (Figure 6C and D). Our data are in agreement with a previous study that showed the ROS scavenger NAC inhibited the phosphorylation of ERα (Papa and Germain, 2011). As ERα at serine 167 is reported to be phosphorylated by AKT (Papa and Germain, 2011), the implications of these findings suggest that E2-induced phosphorylation of ERα may be regulated by ROS via AKT.

Next, we analysed the effect of the antioestrogen TAM on cell cycle gene CDC25C that we previously showed was a target of NRF-1 in E2-treated MCF-7 cells. MCF-7 cells treated with TAM showed an increase in the mRNA levels of CDC25C compared with vehicle control cells (Figure 6E). Our findings were consistent with a previous report that showed, at the molecular level, TAM recapitulates the E2-induced cell cycle gene expression in MCF-7 cells (Hodges *et al*, 2003). The rise in CDC25C mRNA levels in both E2- and TAM-treated cells seems to be related to the ROS generation because cotreatment with the ROS scavenger ebselen inhibited their effect on CDC25C expression (Figure 6E). We also observed a decrease in E2-induced CDC25C mRNA levels by cotreatment with TAM, and this inhibitory effect of TAM was partially reversed with the ebselen cotreatment. Tamoxifen alone in the absence of E2 functions largely as an oestrogen agonist on oestrogen target genes in MCF-7 cells and this may explain its actions, similar to E2, in producing ROS, oxidation of PTEN, and induction of CDC25C mRNA levels (Hodges *et al*, 2003; Shou *et al*, 2004; Penny and Roy, 2013). These findings together suggest that ROS may also have an important role in antioestrogen-mediated growth inhibition of breast cancer cells exposed to TAM.

ROS-dependent localisation of nuclear p27 regulates E2-induced growth of MCF-7 cells. Recently, it has been reported that the cyclin-dependent kinase inhibitor 1B (p27^{Kip1}), a key protein in the decision between proliferation and cell cycle exit, is regulated by ROS-mediated redox signalling (Ibañez *et al*, 2012). Phosphorylation

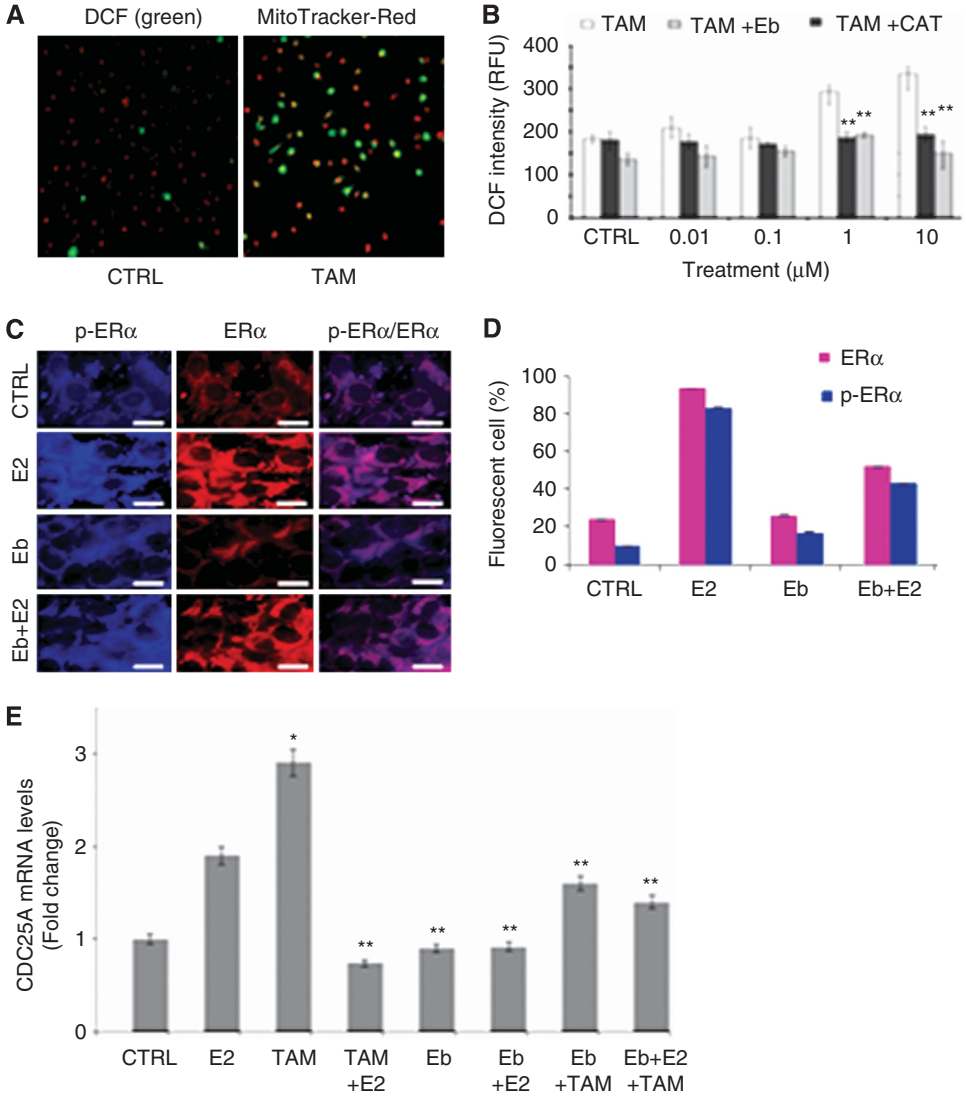

Figure 6. Endogenous ROS regulates antioestrogen effect of TAM-induced gene expression and ER phosphorylation. MCF-7 cells were treated for 30 min with either antioestrogen, tamoxifen (TAM), or E2 (367 pM). (**A**) Treatment with TAM (1 μM) increased oxidation of DCF (green). Mitochondria were labelled with MitoTracker Red. Colocalisation of both probes (yellow) was used as a marker of mitochondrial. (**B**) Analysis of TAM-induced ROS by the DCF assay. Values in the graph show significant inhibition of TAM-induced oxidation of DCF by treatment with ROS scavengers, 20 μM ebselen (Eb), or 500 μg ml^{-1} of PEG-catalase (PEG-CAT). (**C**) Comparison of the effect of Eb on the phosphorylation of ERα (p-ERα) in E2-treated MCF-7 cells. Representative images show Eb reduced the level of p-ERα (blue) in E2-treated MCF-7 cells. Specificity of p-ERα antibody to the ERα was determined by colocalisation of p-ERα antibody (blue) and anti-ER antibody (red) resulting in merged photo in pink colour. (**D**) Graph shows reduced number of E2-treated MCF-7 cells stained with anti-p-ERα antibody when pretreated with Eb. Values in the graph represent the number of ERα and p-ERα fluorescent cells counted and expressed as %. (**E**) Analysis of TAM-induced CDC25C mRNA expression. Graph indicates significant reduction in E2-induced gene expression by TAM and/or Eb treatment. The relative mRNA levels measured for each gene were normalised to 18S RNA. The quantitative values are mean ± s.d. Data shown are representative of three independent experiments. *$P<0.05$, significantly different from control (CTRL); **$P<0.05$, significantly different from E2.

and subcellular localisation of this nuclear regulatory protein are regulated by ROS-mediated AKT signalling. The nuclear localisation signal of p27 contains an AKT consensus site at threonine 157, and phosphorylation of this threonine residue on p27 by AKT inhibits p27's import to the nucleus. This, in turn, prohibits p27 from inhibiting cell proliferation. When p27 is in the cytoplasm, it aids in the assembly of cyclin D1/cdk4, which furthers cell proliferation. When the PI3K pathway has been activated, as it is in human cancers, it has been found that p27 concentrations decrease in the nucleus. This effect is reversed by PTEN. Overexpression of PTEN increases p27 levels, inhibits the phosphorylation of AKT, and through these mechanisms inhibits cell growth in MCF-7 cells (reviewed in Penny and Roy, 2013). Based on these studies, p27 may also be affected by ROS-mediated inactivation of PTEN in E2-exposed MCF-7 cells. We used immunofluorescent confocal microscopy to determine the effect that E2-induced ROS had on the phosphorylation of T157 in p27 and subcellular localisation of p27. In serum-starved MCF-7 cells, both the phosphorylated p27 at T157 and p27 were primarily detected within the nucleus; however, both p27 and phospho-p27 at T157 were predominantly detected in the cytoplasm in E2-treated MCF-7 cells (Figure 7A). The intensity of phosphorylated p27 at T157 was remarkably high in the E2 treatment group compared with the vehicle-treated control and was reduced by cotreatment with ebselen (Figure 7B). In MCF-7 cells treated with only ebselen, we observed a similar distribution of both phosphorylated p27 at T157 and p27 as observed in the control (Figure 7A). Treatment of MCF-7 cells with erucin, which increases TrxR2 levels and lowers oxidation of Trx, also produced a reduction

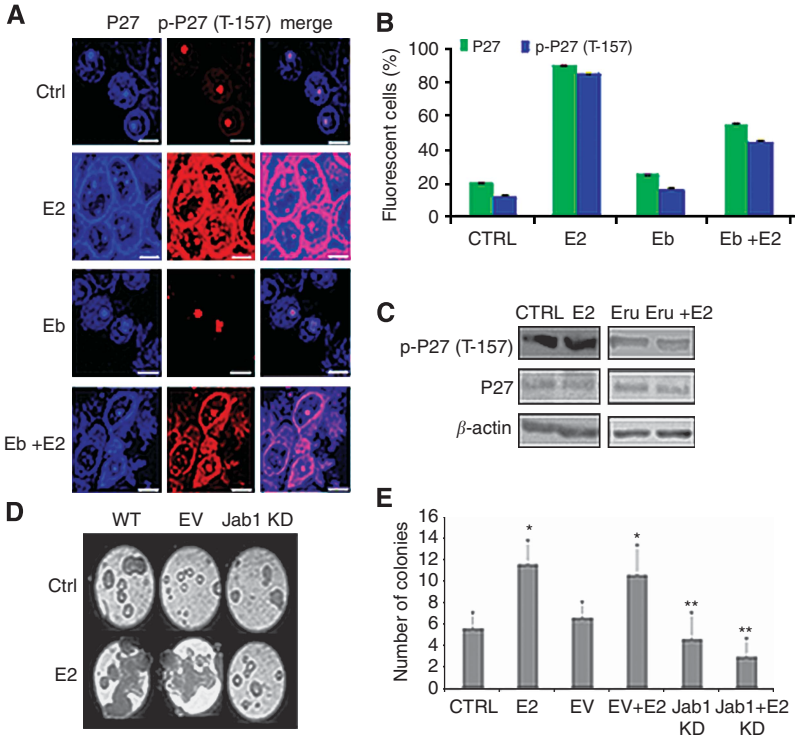

Figure 7. ROS-dependent localisation of nuclear p27 regulate E2-induced growth of MCF-7 cells. MCF-7 cells were treated with E2 (367.1 pM) in the presence of ROS modifiers. (**A**) Analysis of the effect of 20 μM ebselen (Eb) on the cellular localisation of p27 and p-27 in MCF-7 cells for 24 h. MCF-7 cells were stained with anti-p27 and anti-p-p27(T157) antibodies and analysed by confocal microscopy. (**B**) Graph shows reduced number of E2-treated MCF-7 cells stained with anti-p27 or anti-p-p27(T157) antibodies when pretreated with Eb. Fluorescent cells were counted and expressed as %. The quantitative values are mean ± s.d. (**C**) Analysis of the effect of the chemical inducer of TrxR erucin (Eru) has on p27 and p-p27 in E2-treated MCF-7 cells for 16 h. MCF-7 cells were pretreated with 10 μM Eru. Data shown are representative of two independent experiments. (**D**) Colony assay in soft agar of E2-treated MCF-7 cells when treated with Jab1 short hairpin RNa (shRNA). Cells were transfected with a negative regulator of p27 Jab1 shRNA or scrambled control (CTRL) for 48 h. Suppression of Jab1 mRNA expression inhibited E2-induced MCF-7 colonies. (**E**) Bar graph indicates significant inhibition of E2-induced colonies by Jab1 shRNA exposed to E2 (367 pM) for 14 days. Four wells were used for each group and data were expressed as mean of four wells ± s.d. *$P<0.05$, significantly different from control. **$P<0.05$, significantly different from E2. EV, empty vector; KD, knockdown; WT, wild type.

in phosphorylation of p27 at T157 in E2-exposed cells (Figure 7C). These findings combined with our previous data on PTEN and Trx suggests a link between the inactivation of PTEN through its oxidation by ROS that results in enhanced AKT phosphorylation. The phosphorylation of T157 on p27 by an activated AKT may in turn prevent p27 import to the nucleus and results in E2-induced growth of MCF-7 cells via redox signalling. Another mechanism that may contribute to the control of p27 nuclear import that is separate from AKT phosphorylation is via a protein called Jab1. Jab1 protein is known to shuttle p27 from the nucleus to the cytosol as a result of a shift in Trx oxidation during the process of cell proliferation (reviewed in Penny and Roy, 2013). As a result of E2-induced Trx oxidation, more free Jab1 protein should be available to export p27 from the nucleus to cytosol. Thus, we extended our previous studies on p27 to include its regulation by Jab1. We determined whether treatment with Jab1 shRNA could suppress the growth of E2-treated MCF-7 cells. Our results showed that shRNA-mediated Jab1 knockdown significantly inhibited E2-induced MCF-7 colony formation (Figure 7D and E). The growth-suppressive effects of the Jab1-shRNA support a role of Jab1–p27 interactions in the regulation of E2-induced growth of MCF-7 cells.

DISCUSSION

The role of ROS signalling in E2-induced pathogenesis of breast tumor has garnered much attention (Okoh *et al*, 2011; Penny and Roy, 2013). Although ER signalling of cell cycle genes support the growth of breast cancer cells, recent evidence suggests that E2-induced ROS may also contribute in regulating survival, proliferation, and growth of breast cancer cells (Felty *et al*, 2005a, b). In this study, we have demonstrated that E2-induced ROS production may be a necessary step for the signalling cascade that supports E2-induced growth of MCF-7 cells. This process involves oxidative inactivation of PTPs, PTEN, and CDC25A by E2-generated ROS, and a subsequent activation of AKT and ERK pathways that signal downstream nuclear regulatory proteins such as NRF-1 involved in the regulation of cell cycle genes needed for growth of breast cancer cells (see Figure 8). Our study also showed that E2-induced ROS influenced other nuclear proteins such as ERα, p27, and Jab1, which contributed to the growth of MCF-7 cells. The activation of NRF-1, ERα phosphorylation, and the impairment of p27 activity appear to be downstream of E2-induced ROS signalling and the AKT pathway (see Figure 8). These molecules were shown to influence E2-induced anchorage-independent growth of MCF-7 cells. Collectively, these observations indicate a new molecular paradigm by which ROS-inducible signal-transduction pathway(s) may contribute to the E2-mediated growth of breast cancer.

Reactive oxygen species can instigate apoptosis, survival, and proliferation of breast cancer cells, but these individual responses depend on the dose (Okoh *et al*, 2011; Penny and Roy, 2013). The underlying mechanism by which ROS contribute to E2-induced growth of MCF-7 cells remains to be elucidated. Although several nuclear regulatory proteins may be targeted by E2-generated ROS

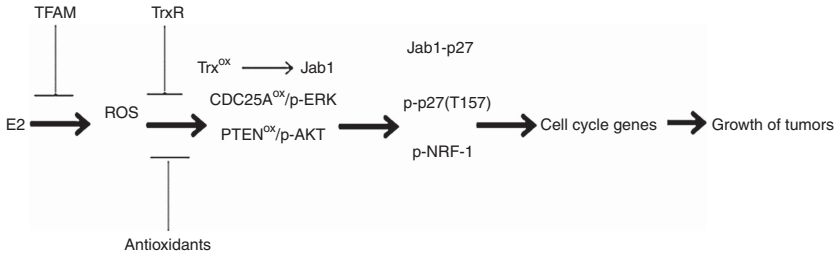

Figure 8. A hypothetical scheme illustrating the role of ROS-induced signalling pathways contributing to E2-induced growth of breast cancer through influencing nuclear regulatory proteins such as NRF-1 and p27. ROS-mediated inactivation of PTPs, CDC25A, and PTEN, presumably leading to the activation of downstream kinases extracellular signal-regulated protein kinases 1 and 2 (ERK1/2), mitogen-activated protein kinase (MAPK), and AKT may regulate E2-induced phosphorylation of nuclear regulatory proteins such as ERα, NRF-1, and p27. This may result in the E2-induced activation of the proliferative stimulation leading to the colony formation. The net effect is E2-induced growth of breast cancer cells. This hypothetical model has support from our data showing E2-induced growth of breast cancer cells can be blocked with the overexpression of ROS-scavenging enzymes catalase or MnSOD, and by suppression of AKT and NRF-1 expression.

in MCF-7 cells, our efforts have focused on the redox-sensitive NRF-1/α-palindrome-binding protein. Motifs bound by ELK1, E2F, NRF-1, and NFY positively correlate with malignant progression of breast cancer (Niida *et al*, 2008). Similarly, our previous study showed that NRF-1 gene expression significantly increases with the progression of breast tumor grades (Kunkle *et al*, 2009). Some of the same mitogenic pathways that are sensitive to ROS levels and E2 are also directly regulated by NRF-1 (Okoh *et al*, 2011). NRF-1 is known to mediate the cellular response to oxidative stress by regulating the expression of genes involved in the cell cycle, DNA repair, cell apoptosis, and mitochondrial biogenesis. However, how ROS through the redox signalling pathway regulate NRF-1 activity in breast cancer cells remains to be elucidated. In this study, we investigated redox signalling pathways that not only activated NRF-1 but were also responsive to exposures to both E2 and ROS. The activation of NRF-1 was studied in the context of the upregulation of cell cycle genes involved in the growth of E2-dependent breast cancer cells. Hydrogen peroxide has been shown to oxidise and thereby inactivate PTEN (Lee *et al*, 2002), which would suggest that increased H_2O_2 formation upon E2 treatment may also affect PTEN activity in MCF-7 cells. Our data showed a dose-dependent increase in the levels of oxidised PTEN after H_2O_2 treatment. In the MCF-7 cells, E2 had similar effects on PTEN oxidation and a cotreatment with ROS scavenger ebselen inhibited this effect, which indicates a contribution from the ROS generated from E2 treatment. Furthermore, lowering intracellular H_2O_2 levels by the overexpression of CAT and by treatment with ROS scavengers inhibited E2-induced phosphorylation of AKT, a downstream target of PTEN/PI3K pathway. The ability of E2 and ROS to induce phosphorylation of AKT may be attributed to the oxidation of PTEN, which is a PI3K inhibitor. The reversible inactivation of PTEN by E2-induced ROS may be a key component of AKT activation. We further tested our concept using another PTP, CDC25A. Our results showed that H_2O_2 or E2 treatment of MCF-7 cells produced oxidised and inactivated CDC25A. This inactivation was prevented by a cotreatment with ROS scavenger NAC. As CDC25A is a PTP known to interact with ERK (Wang *et al*, 2005), E2-induced ROS-mediated inactivation of CDC25A could lead to a higher level of phosphorylated ERK. Thus, it is biologically plausible that the inactivation of CDC25A by E2-induced ROS is responsible for ERK phosphorylation in MCF-7 cells. This observation is consistent with our finding of PTEN oxidation, and with earlier reports suggesting that ROS could reversibly modify the redox state of specific cysteine residues in PTPs and make them inactive. These findings have important implications for understanding the molecular mechanisms by which the redox-sensitive molecules AKT or ERK may participate in E2-mediated signalling to NRF-1. NRF-1 was reported to be a substrate of AKT and activation of AKT controls translocation of NRF-1 to the nucleus. This observation is based on a study in which the translocation of NRF-1 to the nucleus occurred in PTEN-deficient cells and was abrogated when the PI3K pathway was blocked, inactivating AKT (Piantadosi and Suliman, 2006). Our study confirmed that NRF-1 is a direct substrate of AKT in the MCF-7 cells. Serine residues 97, 108, and 116 are the major sites in NRF-1 that are phosphorylated by AKT. Exposure of MCF-7 cells to E2 not only upregulated NRF-1 expression but it also induced phosphorylation of NRF-1 by AKT kinase in a redox-dependent manner. Treatment of cells with ROS modulators or RNAi of NRF-1 prevented E2-induced NRF-1 expression and phosphorylation. These findings show that AKT catalyses NRF-1 phosphorylation in E2-treated MCF-7 cells through an ROS-mediated signalling pathway. Our current study also showed that silencing of NRF-1 or AKT expression reduced MCF-7 colony formation. To examine the effect of ROS production in the transcriptional activation of NRF-1 target genes, we evaluated the effects of ROS scavengers on NRF-1 binding to the promoters of the cell cycle genes: *PRC1*, *PCNA*, *cyclin B1*, *CDC2*, and *CDC25C*. Exposure of MCF-7 cells to E2 increased the binding of NRF-1 to promoters of these cell cycle genes, and this E2 effect was inhibited by the overexpression of H_2O_2 scavenger CAT. To further analyse the mechanism of ROS in regulating cell cycle genes, we studied the effect of ROS scavengers on mRNA expression of NRF-1-regulated cell cycle genes and found that E2-induced expression of these cell cycle genes was also inhibited by the overexpression of H_2O_2 scavenger CAT. These data suggest that ROS regulate E2-induced transcriptional activation of cell cycle genes through NRF-1 modulation. Taken together, these observations strongly support our concept that ROS-inducible PI3K-AKT signalling pathway acts as one of the main signal-transduction pathways triggering NRF-1 activation and subsequent NRF-1-mediated transcription of cell cycle genes in response to E2 exposure (Figure 8). Our findings suggest that ROS modulators may be useful agents to inhibit the E2-induced tumor phenotype and have the potential for further therapeutic development.

In addition to NRF-1 signalling, ROS may also influence other E2-regulated nuclear proteins such as ERα and p27. AKT phosphorylates both ERα and p27. Our findings revealed that E2-induced phosphorylation of ERα may be dependent on ROS signalling because the ROS scavenger ebselen inhibited E2-induced ERα phosphorylation. Although ERα is believed to regulate E2-induced NRF-1 expression in MCF-7 cell line (Ivanova *et al*, 2011), our data indicate that E2-induced ROS are also essential for phosphorylation of both ERα and NRF-1. Furthermore, our study revealed that AKT-mediated phosphorylation of p27 inhibited p27 import to the nucleus. The significance of this finding is that E2-induced ROS signalling may allow for the growth of MCF-7 cells

by an additional mechanism such as redox-mediated sequestering of p27 away from the nucleus, which in turn allows the cell cycle to progress without interference by the cell cycle inhibitory protein p27. In this study, we found that reducing the level of oxidised Trx by overexpression of its reductase TrxR2 blocked phosphorylation of T157 in p27 and prevented the cytosolic accumulation of p-p27(T157) in E2-treated MCF-7 cells. Furthermore, we showed that shifting the redox state of Trx to a more reduced state resulted in decreased MCF-7 colony formation in E2-exposed cells as well as decreased phosphorylation of p27 at T157, which helped to retain the inhibitory p27 protein in the nucleus. Trx has been shown to compete with p27 for binding with Jab1 (Pan *et al*, 2012; Penny and Roy, 2013), and this negatively regulates p27 degradation. We observed that altering the redox state of cells by overexpression of Trx reductase inhibits E2-induced *colony* formation of MCF-7 cells. Decreasing Jab1 expression also led to a decrease in E2-induced *colony* formation. Taken together, our findings suggest that E2-induced growth of MCF-7 cells may not only be regulated via NRF-1. Instead, other nuclear regulatory proteins such as ERα may also be activated in a similar manner by redox-sensitive kinases downstream of PTPs such as AKT. Besides transcription factors, cell cycle inhibitory proteins such as p27 may also be regulated by redox signalling via sequestering p27 away from the nucleus that allows for E2-induced cell growth.

In summary, the major novel findings of this study illustrate that the activation of NRF-1 and impairment of p27 by E2 are dependent on ROS formation. 17β-Oestradiol generated ROS-inactivate PTEN and CDC25A, which may activate AKT and ERK1/2, respectively. Activated AKT and ERK1/2 phosphorylate NRF-1 leading to the translocation of NRF-1 to the nucleus, where it activates the transcription of cell cycle genes that control E2-mediated anchorage-independent growth of MCF-7 cancer cells. Findings of this study not only provide a new paradigm in understanding the mechanism of E2-dependent growth of malignant breast cancer cells but it also provides important information for the design of new antioxidant-based drugs for the prevention and treatment of oestrogen-dependent breast cancer.

ACKNOWLEDGEMENTS

This work was in part supported by a DOD Grant (W81XWH-07-1-0417) and a VA MERIT Review (VA BX001463) Grant to DR.

CONFLICT OF INTEREST

The authors declare no conflict of interest.

REFERENCES

Aapro M, Eliason JF, Krauer F, Alberto P (1987) Colony formation *in vitro* as a prognostic indicator for primary breast Cancer. *J Clin Oncol* **5**: 890–896.

Arteaga E, Villaseca P, Bianchi M, Rojas A, Marshall G (2003) Raloxifene is a better antioxidant of low-density lipoprotein than estradiol or tamoxifen in postmenopausal women *in vitro*. *Menopause* **10**: 142–146.

Deruy E, Gosselin K, Vercamer C, Martien S, Bouali F, Slomianny S, Bertout J, Bernard D, Pourtier A, Abbadie C (2010) MnSOD upregulation induces autophagic programmed cell death in senescent keratinocytes. *PLoS One* **5**: e12712.

Felty Q, Xiong WC, Sun D, Sarkar S, Singh KP, Parkash J, Roy D (2005a) Estrogen-induced mitochondrial reactive oxygen species as signal transducing messengers. *Biochemistry* **44**: 6900–6909.

Felty Q, Singh KP, Roy D (2005b) Estrogen-induced G(1)/S transition of G(0)-arrested estrogen-dependent breast cancer cells is regulated by mitochondrial oxidant signaling. *Oncogene* **24**: 4883–4893.

Herzig RP, Scacco S, Scarpulla RC (2000) Sequential serum-dependent activation of CREB and NRF-1 leads to enhanced mitochondrial respiration through the induction of cytochrome *c*. *J Biol Chem* **275**: 13134–13141.

Hodges LC, Cook JD, Lobenhofer EK, Li L, Bennett L, Bushel PR, Aldaz CM, Afshari CA, Walker CL (2003) Tamoxifen functions as a molecular agonist inducing cell cycle-associated genes in breast cancer cells. *Mol Cancer Res* **1**: 300–311.

Ibañez IL, Bracalente C, Notcovich C, Tropper I, Molinari BL, Policastro LL, Durán H (2012) Phosphorylation and subcellular localization of p27Kip1 regulated by hydrogen peroxide modulation in cancer cells. *PLoS One* **7**: e44502.

Ivanova MM, Luken KH, Zimmer AS, Lenzo FL, Smith RJ, Arteel MW, Kollenberg TJ, Mattingly KA, Klinge CM (2011) Tamoxifen increases nuclear respiratory factor 1 transcription by activating estrogen receptor beta and AP-1 recruitment to adjacent promoter binding sites. *FASEB J* **25**: 1402–1416.

Lam EWN, Zwacka R, Engelhardt JF, Davidson BL, Domann FE, Van T, Oberley LW (1997) Adenovirus-mediated manganese superoxide dismutase gene transfer to hamster cheek pouch carcinoma cells. *Cancer Res* **57**: 5550–5556.

Kallio A, Zheng A, Dahllund J, Heiskanen KM, Härkönen P (2005) Role of mitochondria in tamoxifen-induced rapid death of MCF-7 breast cancer cells. *Apoptosis* **10**: 1395–1410.

Kunkle B, Felty Q, Trevino F, Roy D (2009) Meta-analysis of breast cancer microarray data identifies upregulation of NRF1 expression in human breast carcinoma. Proceedings of the 18th World IMACS/MODSIM Congress. Available at: http://www.mssanz.org.au/modsim09/B6/kunkle_B6a.pdf.

Lazo JS, Aslan DC, Southwick EC, Cooley KA, Ducruet AP, Joo B, Vogt A, Wipf P (2001) Discovery and biological evaluation of a new family of potent inhibitors of the dual specificity protein phosphatase Cdc25. *J Med Chem* **44**: 4042–4049.

Lee SR, Yang KS, Kwon J, Lee C, Jeong W, Rhee SG (2002) Reversible inactivation of the tumor suppressor PTEN by H_2O_2. *J Biol Chem* **277**: 20336–20342.

Niida A, Smith AD, Imoto S, Tsutsumi S, Aburatani H, Zhang MQ, Akiyama T (2008) Integrative bioinformatics analysis of transcriptional regulatory programs in breast cancer cells. *BMC Bioinform* **9**: 404–410.

Marino M, Acconcia F, Trentalance A (2003) Biphasic estradiol-induced AKT phosphorylation is modulated by PTEN via MAP kinase in HepG2 cells. *Mol Biol Cell* **14**: 2583–2591.

Migliaccio A, Di Domenico M, Castoria G, de Falco A, Bontempo P, Nola E, Auricchio F (1996) Tyrosine kinase/p21ras/MAP-kinase pathway activation by estradiol-receptor complex in MCF-7 cells. *EMBO J* **15**: 1292–1300.

Okoh V, Deoraj A, Roy D (2011) Estrogen-induced ROS mediated redox signaling contributes in the development of breast cancer. *Biochem Biophys Acta* **1815**: 115–133.

Okoh VO, Felty Q, Parkash J, Poppiti R, Roy D (2013) Reactive oxygen species via redox signaling to PI3K/AKT pathway contribute to the malignant growth of 4-hydroxy estradiol-transformed mammary epithelial cells. *PLoS One* **8**: e54206.

Pan Y, Zhang Q, Tian L, Wang X, Fan X, Zhang H, Claret FX, Yang H (2012) Jab1/CSN5 negatively regulates p27 and plays a role in the pathogenesis of nasopharyngeal carcinoma. *Cancer Res* **72**: 1890–1900.

Papa L, Germain D (2011) Estrogen receptor mediates a distinct mitochondrial unfolded protein response. *J. Cell Sci* **124**: 1396–1402.

Parkash J, Felty Q, Roy D (2006) Estrogen exerts a spatial and temporal influence on reactive oxygen species generation that precedes calcium uptake in high-capacity mitochondria: implications for rapid nongenomic signaling of cell growth. *Biochemistry* **45**: 2872–2881.

Penney RB, Roy D (2013) Thioredoxin-mediated redox regulation of resistance to endocrine therapy in breast cancer. *Biochim Biophys Acta* **1836**: 60–79.

Piantadosi CA, Suliman HB (2006) Mitochondrial transcription factor A induction by redox activation of nuclear respiratory factor 1. *J Biol Chem* **281**: 324–333.

Shou J, Massarweh S, Osborne CK, Wakeling AE, Ali S, Weiss H, Schiff R (2004) Mechanisms of tamoxifen resistance: increased estrogen receptor-HER2/neu cross-talk in ER/HER2-positive breast cancer. *J Natl Cancer Inst* **96**: 926–935.

Turrens JF, Alexandre A, Lehninger AL (1985) Ubisemiquinone is the electron donor for superoxide formation by complex III of heart mitochondria. *Arch Biochem Biophys* **237**: 408–414.

Wang W, Wang S, Howie AF, Beckett GJ, Mithen R, Bao Y (2005a) Sulforaphane, erucin, and iberin up-regulate thioredoxin reductase 1 expression in human MCF-7 cells. *J Agric Food Chem.* **53**: 1417–1421.

Wang Z, Zhang B, Wang M, Carr BI (2005) Cdc25A and ERK interaction: EGFR-independent ERK activation by a protein phosphatase Cdc25A inhibitor, compound 5. *Physiology* **204**: 437–444.

Wang C, Li Z, Lu Y, Du R, Katiyar S, Yang J, Fu M, Leader JE, Quong A, Novikoff PM, Pestell RG (2006) Cyclin D1 repression of nuclear respiratory factor 1 integrates nuclear DNA synthesis and mitochondrial function. *Proc Natl Acad Sci USA* **103**: 11567–11572.

Watson WH, Pohl J, Montfort WR, Stuchlik O, Reed MS, Powis G, Jones DP (2003) Redox potential of human thioredoxin 1 and identification of a second dithiol/disulfide motif. *J Biol Chem* **278**: 33408–33415.

Wu Y, Kwon KS, Rhee SG (1998) Probing cellular protein targets of H_2O_2 with fluorescein-conjugated iodoacetamide and antibodies to fluorescein. *FEBS Lett* **440**: 111–115.